Composite Bicycle Fork Design for Vacuum Assisted Resin Transfer Moulding

by
MARC-ANDRÉ OCTEAU

Department of Mechanical Engineering
McGill University, Montreal

A Thesis Submitted to the Faculty of Graduate Studies and Research in Partial Fulfillment of the Requirements of the Degree of Master of Engineering

0-612-70247-2

ABSTRACT

The carbon fork developed for this thesis is a lightweight fork intended for the road racing athletes and amateurs. The work performed for this thesis includes geometrical and structural design of the fork but also concentrates on developing and optimizing a manufacturing process to create a complete solution for composite fabrication using vacuum assisted resin transfer moulding (VARTM). In the past many research projects concentrated on structural design and finite element analysis but failed to show satisfactory practical results due to poor manufacturing method for prototypes. This thesis emphasizes the development of the fabrication process. The stages for this thesis consist of analyzing previous work done on a carbon fibre fork and, from there, creating and developing a new fork whose weight will be reduced and performance increased. Using this new design, a new custom manufacturing process is implemented for VARTM. The final stage consists of producing prototypes and evaluating their performance and resistance under static and fatigue loadings.

RÉSUMÉ

La fourche de vélo en carbone développée pour cette thèse est destinée à l'usage des athlètes et coureurs amateurs. Les travaux encourus dans cette thèse incluent le design géométrique et structurel de la fourche. De plus, la recherche se concentre aussi sur le développement et l'optimisation d'un procédé de manufacture pour ainsi créer une solution complète pour la fabrication de pièces en matériaux composites utilisant l'injection par transfert de résine sous vide (VARTM.) Dans le passé plusieurs projets de recherches se sont concentrés essentiellement sur le design géométrique et l'analyse par éléments finis. Cependant, ces derniers échouaient dans la démonstration pratique due à des méthodes de manufacture incomplètes pour la production de prototypes. Cette thèse insiste sur le développement du procédé de fabrication par VARTM. Les étapes pour compléter cette recherche incluent l'analyse des recherches précédentes portant sur les fourches en fibre de carbone et la création et le développement d'une nouvelle fourche avec un poids allégé et des performances améliorées. Partant du design, un nouveau procédé de fabrication spécialement adapté à la fourche est créé pour le VARTM. La dernière étape consiste à fabriquer des prototypes et à évaluer leurs performances aux cas de charges statiques et en fatigue.

AKCNOWLEDGEMENTS

I want to thank my thesis supervisor, Dr. Larry Lessard, who became a good friend through the course of my studies. I also thank everybody at McGill University who help me during my thesis, especially Mathieu Dakowski who shared my pain when I was writing my thesis, Brock Leong for his great help with the test machine, Sacha Tibbets who showed me how to use a CNC and helped me make the mould and Spiro Mitsialis for his indispensable help with the many computer problems. Special thanks to the whole Serotta crew, especially Ben who supported me during my years spent at developing my thesis project. Jérôme LeCorvec from Kaizen Technologies for introducing me to RTM and to the industrial world of composites. Merci beaucoup à mère, Claudette, qui a été un vrai support moral durant toutes ces années. À mon père qui m'a supporté pendant mon travail. Merci à vous tous qui avez partagés ma vie et m'avez aidés à réaliser mes rêves.

TABLE OF CONTENTS

LIST OF FIGURES

LIST OF TABLES

Chapter 1: Introduction

1.1 Motivation

The use of composite materials in the bicycle industry has increased considerably in the last 10 years. Prototypes of composites frames and bicycles components have made their way into production and now many can be seen on the market. The market competition has seemingly increased and now composite parts are asked to meet high standards of performance and be extremely lightweight while remaining at a competitive price with metallic components [1-2].

1.2 Objectives

The objectives for this thesis are based on the redesign of an existing carbon fibre fork commercialized by Serotta Competition Bicycles. The main objective is to develop a new structure for the carbon fibre fork with manufacturing in mind. The new design is oriented in order to reduce the fork weight by 25% while keeping the same rigidity and ride quality. The fatigue life of the fork has to match the life of other high performance carbon forks on the market. The design also has to be easily produced at minimum cost with high quality and repeatability. The performance of the fork and the consistency of the manufacturing method will be validated with static and fatigue loading experiments.

Chapter 2: Product Review

2.1 Bicycle Review

The subject of this thesis is based on a bicycle fork. It is then important to introduce the general structure and definition of a complete bicycle to understand the interaction between the fork and its surroundings.

> **Bicycle,** vehicle consisting of two wheels fixed in tandem to a frame, steered by handlebars, and propelled by an arrangement of pedals and gears driven by the feet. The name of the modern vehicle dates from 1869. Various precursors of this machine were known as *vélocipèdes,* from a French name dating from the late 18th century. [3]

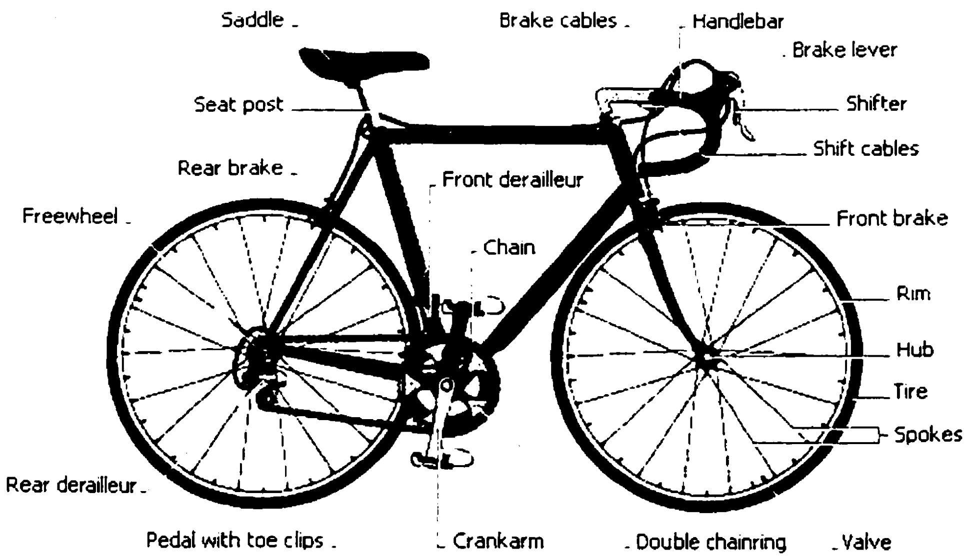

Figure 2.1: Nomenclature for a Bicycle and its Components [3]

Historically, steel has been use intensively in the making of bicycle and its components. Steel tubing was developed over the years to perform adequately for the human body in term of reaction, stability and dampening. [4] High quality steel bicycle frames and forks are well renowned for their great response and ride quality. However the demanding world of racing is asking for lighter structures than what can be achieved with steel. Aluminium is now commonly used in making extremely light frames and forks but the nature of this material leads to exceptionally stiff and uncomfortable pieces of equipment to ride on. Lately the most promising option has been composite materials with the ability to tune a designed part to specific behaviours.

2.2 Bicycle Fork Review

The fork is a critical component of the bicycle. It is connected to the frame through bearings. The fork is a major component in the ride quality of the bicycle. The response of the bicycle to the road and during turning depends greatly on the stiffness and damping of the fork. Furthermore, the fork undergoes many types of load during use. Failure of the fork would be catastrophic, so extreme caution has to be put into testing to assure high impact resistance and long fatigue life. It is also preferable that the mode of failure of the fork be slow and shows signs of failure before breaking.

In this research, a composite fork will be the focus of the study. The design and study of a fork ask for a nomenclature of the different regions of the fork as well as specific names for dimensioning the fork itself and the fork relative to the bicycle frame, as shown in figures 2.2, 2.3 and 2.4.

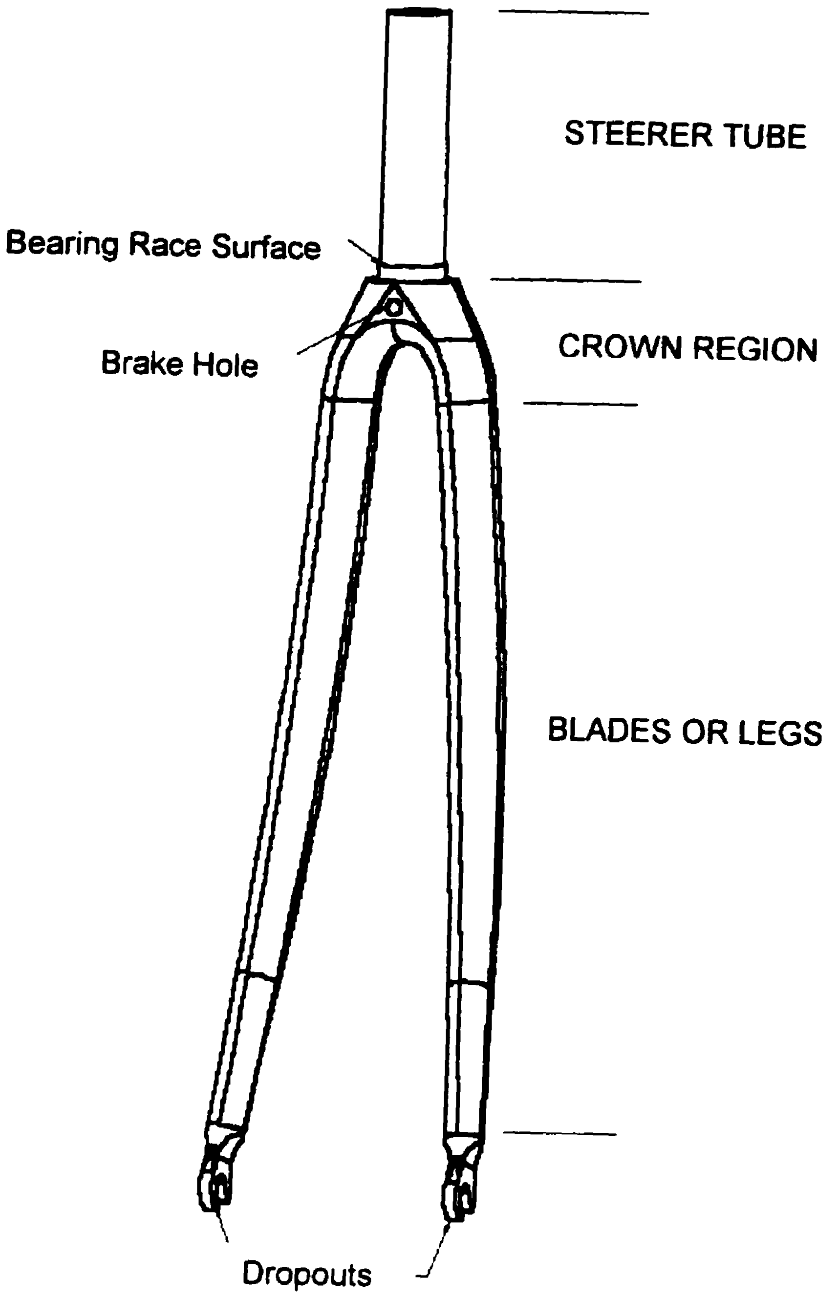

Figure 2.2: Nomenclature for a Bicycle Fork

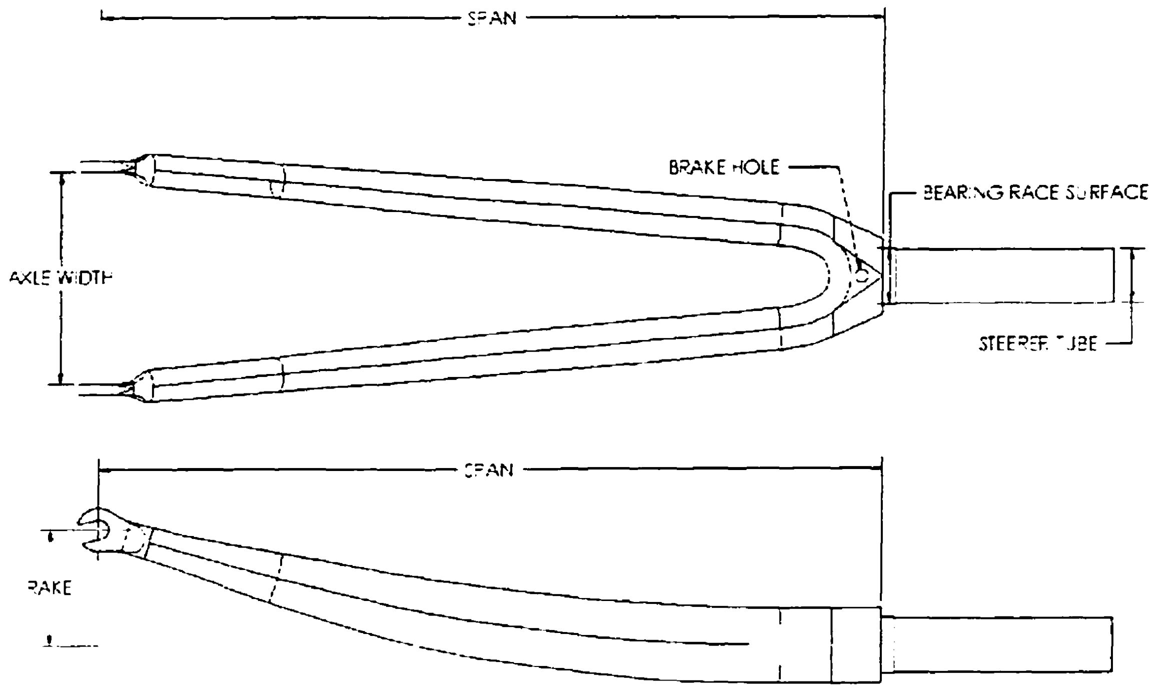

Figure 2.3: Fork Dimension Description

Bicycle fork dimensions are described with four major dimensions: steerer tube diameter, span (also called fork length), rake and axle width. The steerer tube diameter and axle width are industry standards. The steerer diameter is either 1 inch or 1.125 inches and axle width either fits a road or mountain wheel axle. The rake and the span are variable. Companies produce different dimensions. The span depends on the size of the wheel used. The rake however can be tuned to give particular ride characteristics.

The rake of the fork influences the trail of a bicycle (see figure 2.4). The trail is: "the distance between the wheel axle and the steering axis where they intersect the ground." [5] The trail of a bicycle has a direct consequence on the stability of the bicycle. However it is almost impossible to define a mathematical equation to describe bicycle steering. By experience, the rake on road bicycle is between 40 and 60 mm [1]. A longer rake provides more stability and is usually used on touring bikes while a shorter one offers a more responsive ride and is used on racing bicycles.

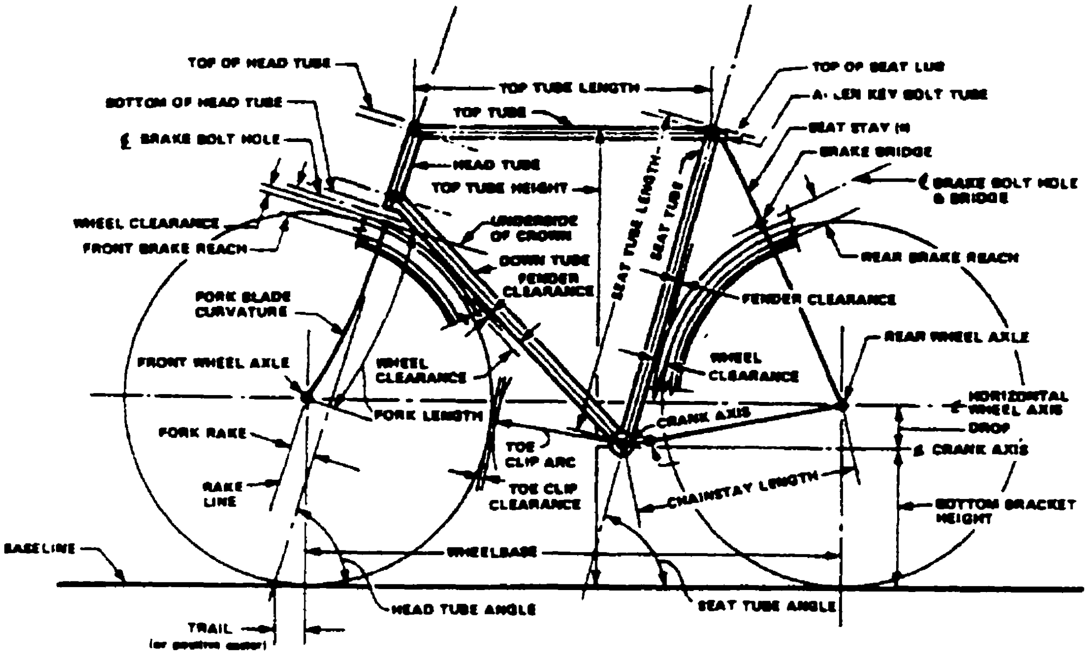

Frameset Geometry and Principle Design Elements by Richard Talbot, from *Designing and Building Your Own Frameset.*

Figure 2.4: Nomenclature for Bicycle and Fork Dimensions [4]

Two more fork dimensions are used to define the size of a fork and are relative to the bicycle frame geometry. The first dimension is the angle of the fork steering column with the ground. This angle is defined by the bicycle head tube angle as shown in figure 2.4. The length of the steerer tube is the last dimension to describe the fork geometry. The length of the head tube and the choice of headset-stem combination (see headset descriptions below) define that steerer tube length as the fork steerer is cut to fit the assembly upon installation on the frame.

Two different types of forks exist on the market: threaded and threadless forks. The difference, as mentioned in the name, resides in the type of steerer tube used. The steerer tube configuration dictates which type of headset is used on the bicycle. The headset is the bearing assembly mounted on the steering column for smooth handling. The two headset styles are specified for the type of steerer column: threaded or threadless (also called Aheadset [6] style which refers to the company that invented that style). Different types of stems are used depending on the type of steerer tube/headset combination.

For the first type, threaded, a bearing race is press fit on the fork crown and the steerer tube is threaded for adjusting the bearing tension. The stem is assembled to the fork inside the steerer with a wedge system. This wedge system tends to damage the steerer tube because it causes unsymmetrical stresses around the tube. This is the "traditional" method for mounting a fork and is the main reason why it is still in use. Conventionalist cyclists tend to prefer the threaded fork mainly because of style.

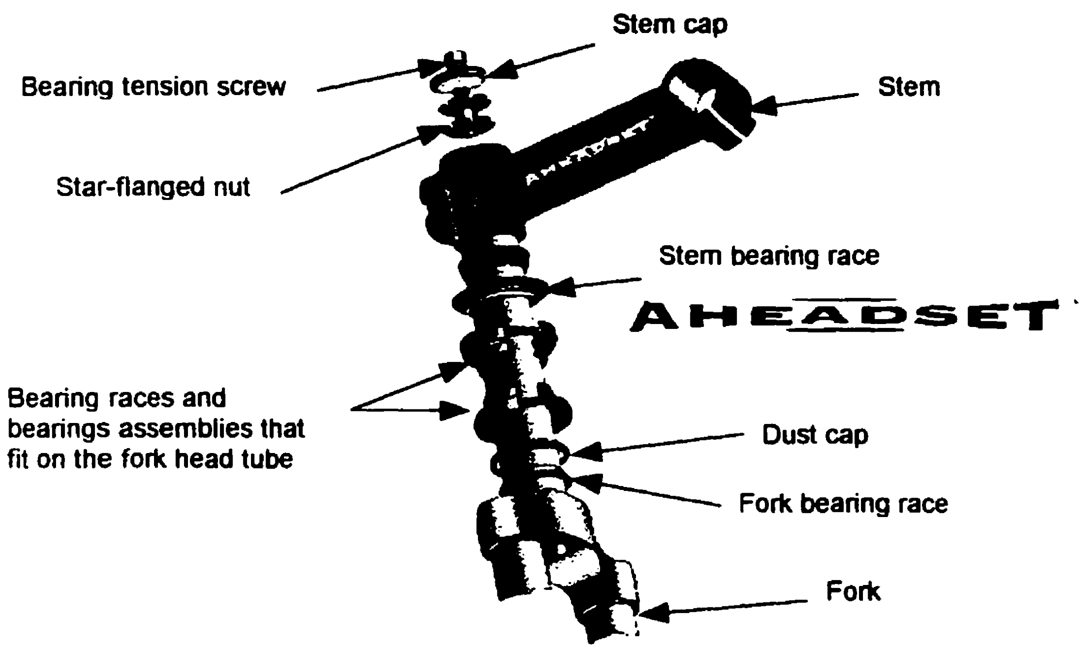

Figure 2.5: Threadless (or Aheadset) Bearing Style. [6]

For the second type, threadless or Ahead, a bearing race is press fit on the fork shoulder (same as threaded fork) but the steerer tube is not threaded for adjusting the bearing tension. A stem is clamped over the steerer tube. Fitting a nut in the steerer tube and tensioning a screw placed over a stem cap adjust the bearing tension. This style offers the advantage of putting only hoop stresses on the steerer tube when the stem is clamped. Also the height of the stem can be easily adjusted by placing spacers between the bearing race and the stem.

2.3: Composites Review

The main subject of this thesis is the study of manufacturing methods to produce a bicycle fork. The nature of composite materials and the different manufacturing methods available for composite fabrication have to be well known before starting the design process.

> Composite Materials
>
> Composite materials are a unique class of materials made by combining two or more materials to obtain a new material that has properties from both components. These materials offer some significant advantages over traditional materials in many structural applications. These advantages are due to the ability to select various combinations of fiber reinforcement and resin material. A composite material can be selected from this spectrum to provide the optimal choice to meet application requirements. [7]

What is a Composite?

Composite materials are composed of a matrix material reinforced with any of a variety of fibers made from ceramics, metals, or polymers. The reinforcing fibers are the primary load carriers of the material, with the matrix component transferring the load from fiber to fiber. Reinforcement of the matrix material may be achieved in a variety of ways. Fibers may be either continuous or discontinuous. Reinforcement may also be in the form of particles. The matrix material is usually one of the many available engineering plastics/polymers. Selection of the optimal reinforcement form and material is dependent on the property requirements of the finished part. [7]

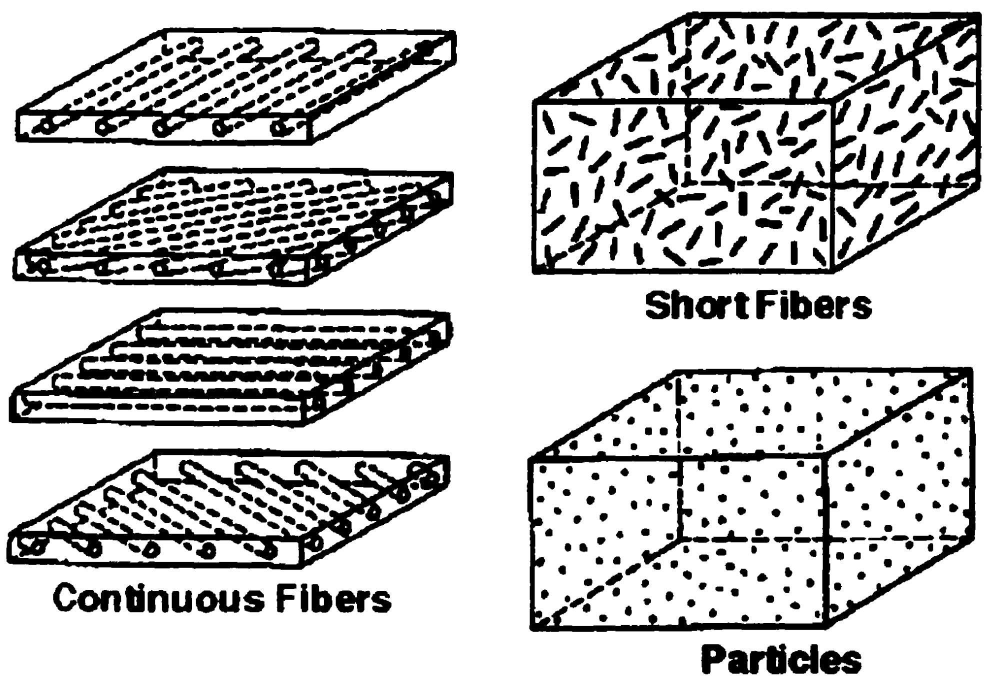

Figure 2.6: Composites Reinforcement Material Types [7]

2.3.1: Matrices

The matrices are generally composed of plastic/polymer. Ceramic and metal matrices are also available but they necessitate special methods of manufacturing requiring extremely high temperatures of formability that are out of the scope of this study. Plastic matrices are commonly used in composites due to their availability, versatility and ease of process. Plastic polymers are divided in to two major categories: Thermosetting plastics and Thermoplastics.

> Thermoplastics can be repeatedly softened by heating and hardened by cooling. Thermosetting plastics, on the other hand, harden permanently after being heated once.
>
> The reason for the difference in response to heat between thermoplastics and thermosetting plastics lies in the chemical structures of the plastics. Thermoplastic molecules, which are linear or slightly branched, do not chemically bond with each other when heated. Instead, thermoplastic chains are held together by weak van der Waal forces (weak attractions between the molecules) that cause the long molecular chains to clump together like piles of entangled spaghetti. Thermoplastics can be heated and cooled, and consequently softened and hardened, repeatedly, like candle wax. For this reason, thermoplastics can be remolded and reused almost indefinitely.
>
> Thermosetting plastics consist of chain molecules that chemically bond, or cross-link, with each other when heated.

When thermosetting plastics cross-link, the molecules create a permanent, three-dimensional network that can be considered one giant molecule. Once cured, thermosetting plastics cannot be remelted, in the same way that cured concrete cannot be reset. Consequently, thermosetting plastics are often used to make heat-resistant products, because these plastics can be heated to temperatures of 260° C (500° F) without melting. [8]

Some of the different thermosetting plastics and thermoplastics found in the composite industry are the following:

- Thermosetting: Polyurethane, Phenolics, Epoxy resin, Polyester
- Thermoplastic: Polyethylene (PE), Polypropylene (PP), Polystyrene (PS), Polyvinyl Chloride (PVC), Polytetrafluoroethylene (PTFE) or Teflon, Polyamides (PA) (example: Nylon), Polyether-ether-Ketone (PEEK)

For many reasons, the matrix of choice for this project is a thermosetting epoxy. First, epoxies are well known in the domain of high performance composites and are available at relatively low cost when compared to most thermoplastics. Thermoplastics are still under development, are more expensive and require manufacturing techniques involving specialized equipment at high temperatures. This may not be true for industrial thermoplastics, but this research focuses specifically on high performance composites.

Epoxies can be processed at low temperatures, from room temperature up to 450°F. Also, epoxy has many mechanical advantages over other thermosetting matrices [9]:

- Outstanding adhesion (with both fibres and metals)
- Excellent strength

- Excellent fatigue strength
- Excellent corrosion and weather resistance
- Thermal expansion stability during curing

2.3.2 Fibre Material

Fiber, fine hairlike structure, of animal, vegetable, mineral, or synthetic origin. Commercially available fibers have diameters ranging from less than 0.004 mm (0.00015 in) to 0.2 mm (0.008 in) and they come in several different forms: short fibers (known as staple, or chopped), continuous single fibers (monofilament), untwisted bundles of continuous filaments (tow), and twisted bundles of continuous filaments (yarn). Fibers are classified according to their origin, chemical structure, or both. They can be braided into ropes and cordage, made into felts (also called nonwovens), woven or knitted into textile fabrics, or, in the case of high-strength fibers, used as reinforcements in composites—that is, products made of two or more different materials. [10]

The use of composite materials is growing more and more popular and the need to produce recyclable and biodegradable material lead to the use of natural fibres, but herbal fibres usually do not meet the performance requirements and high strength animal fibres like spider web are still in the experimental stage. Therefore, mineral and synthetic fibres are still the most commonly used types of fibres in high performance composite materials.

The most widely used type of fibre in the composite world is a mineral fibre made of glass (Fiberglass). High performance composites, however, require fibres with a higher strength and modulus. Ceramic fibres like aluminium oxide (Al_2O_3), silicon carbide (SiC) and boron carbide (B_4C) were discovered in the 1960's and have better mechanical properties. Ceramic fibres are not very popular because of their higher cost over fibreglass and synthetic fibres.

High strength synthetic fibres, carbon, graphite and aramid (aromatic polyamide also called Kevlar©) are generally used in high performance structures. Those fibres are significantly more expensive than fibreglass, but offer greater mechanical properties. Carbon fibres are made from rayon or acrylic fibres carbonized at temperatures between 1000°C and 2500°C. Graphite fibres are made at temperatures over 2500°C. Graphite shows better properties than carbon, but is offered at a higher cost.

Property	Units	Graphite	Glass	Aramid
Axial Modulus	GPa	230	85	124
Transverse modulus	GPa	22	85	8
Axial Poisson's ratio	-	0.3	0.2	0.36
Transverse Poisson's ratio	-	0.35	0.2	0.37
Axial shear modulus	GPa	22	35.42	3
Axial coefficient of thermal expansion	μm/m/°C	-1.3	5	-5
Transverse coefficient of thermal expansion	μm/m/°C	7	5	4.1
Axial tensile strength	MPa	2067	1550	1379
Axial compressive strength	MPa	1999	1550	276
Transverse tensile strength	MPa	77	1550	7
Transverse compressive	MPa	42	1550	7
Shear strength	MPa	36	35	21
Specific gravity	-	1.8	2.5	1.4

Table 2.1: Typical Properties of Fibres [11]

2.3.3 Composite Material

A part can be made from composite materials only if the fibres and the matrix are combined to form a composite. The action of mixing the matrix with the fibres is called wetting in the nomenclature of composites. Most fibres are surface treated in order to increase the adhesion strength between the fibres and the matrix. One important aspect of composite materials is the volume ratio between the fibres and the matrix in the structure [12]. In order to gain the most from each constituent, the proper amount of matrix has to be added to the fibres and dispersed homogeneously.

Typically for high performance composites, the volume ratio of fibre is between 50 and 70 %. Parts with a volume ratio above 70 % are impractical to manufacture since it would be difficult to wet all the fibres properly. On the lower end, if the volume ratio is below 50 %, the strength of the fibres relative to the matrix is not optimized and the part is not considered to be in the high performance category. For industrial use, the fibre volume ratio varies between 20 and 50 %. The difference between high performance parts and industrial parts can be illustrated by comparing a carbon fibre airplane wing to a fibreglass bathtub.

The material of concern for this research will be continuous fibre in different arrangements. The matrix will be an epoxy with high mechanical properties. The composite combination of the fibres and the epoxy will be at the maximum fibre ratio to achieve high mechanical properties per unit weight.

The composite can be constructed either from separate dry fibres and liquid epoxy or from pre-impregnated (prepreg) fabric. Prepregs are fabrics with a controlled amount of epoxy already mixed with the fibres. In prepregs, the epoxy resin is already combined with the corresponding hardener. The material is mounted on a non-stick backing paper and rolled. It is then kept at low temperature (usually in a freezer at -18°C) to slow the cross-linking process of the polymer. Heating the prepreg in an oven during manufacturing activates the curing process. Most prepregs have relatively short shelf life of six months (in a freezer) for optimal performance.

The format in which the fibres and the matrix are mixed together, either in dry fabric with a separate matrix or in prepreg, dictates which manufacturing process the part will be used.

2.3.4 Manufacturing Methods

The anisotropic behaviour of composites is the key element when defining how a part will be made. Unlike isotropic materials like metals, composite parts cannot be machined to their final shape, but have to be moulded to shape while maintaining the design properties like fibre ratio and fibre orientation. The general procedure for composite manufacturing is called the laminating process, which consists of binding layers of reinforcement material in a matrix. Many processes are available for creating a laminate.

The primary feature is formability. The laminate has to be shaped in a mould. From there, as mentioned earlier, different methods are available to produce a composite part and it will primarily depend on if dry or prepreg fabric is used. The most common techniques of interest for this research are then:

- Prepreg
- Wet Layup
- Infusion
- Resin Transfer Moulding (RTM)

The choice of the method is also influenced by the results sought and by which means the part will be produced.

- Automated Processes or hand layup
- Fibre ratio (percent fibre versus percent matrix)
- Repeatability
- Surface quality
- Void content

- Production time
- Production rate
- Geometric tolerances
- Mechanical properties
- Curing temperature

Wet Layup

Wet layup is the manufacturing method requiring the least equipment. The method is called hand layup in its simplest form, but can evolve into a more complex automated process. The method consists of placing dry fibres in the mould by hand and "wetting" the fibres with a liquid matrix using a brush, a roller or a spatula (See figure 2.7). A variation of this technique involves shooting chopped fibres and the matrix together in the mould with a spray gun (See figure 2.8). The spray gun is fed with resin and spools of continuous fibres and as the fibres go into the gun, they are chopped to desired length and shot into the mould with a pressurized flow of resin (like a paint gun). This technique is used generally for industrial applications with low structural properties like bathtubs and shower cabinets. The "chopper" gun technique can produce higher quality parts when automated. A gun mounted on a robotic arm and fibre-matrix feed can be computerized to control the part thickness in a specified area and the process repeatability for production of structural parts. Bombardier Seadoo™ shells are manufactured using this method [13].

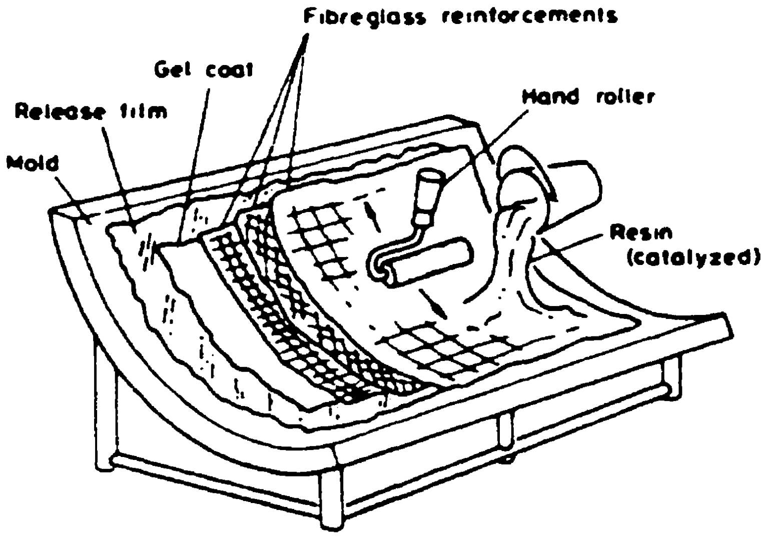

Figure 2.7: Hand Layup Process [14].

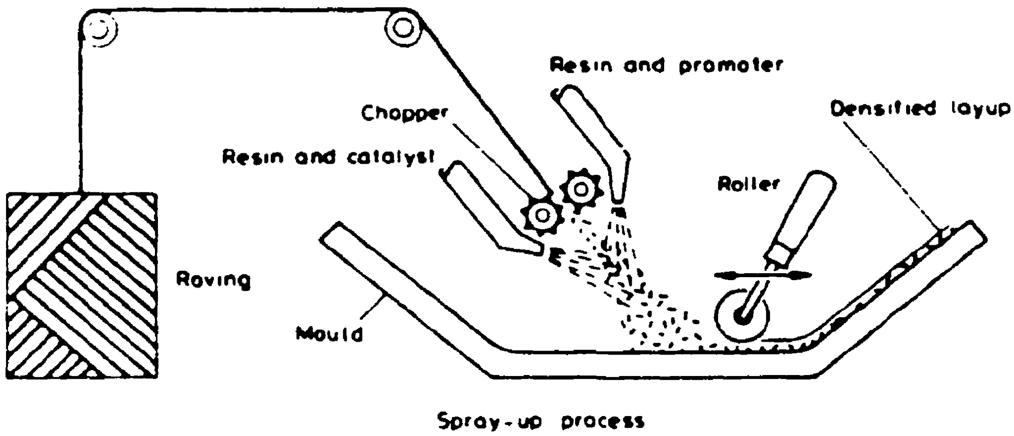

Figure 2.8: Spray Gun Process [14]

The wet layup technique requires an open mould (as opposed to a closed mould). An open mould consists of only the female representative of the external surface of the part. The internal surface is not moulded. A vacuum bag can be placed over the internal surface to apply pressure. A vacuum bag is a thin film of plastic impermeable to gas. It is sealed to the mould with a sealant tape [15]. The vacuum pressure placed on the laminate increases the part quality by removing air bubbles trapped in the resin by pressing the laminate snugly on to the mould. The disadvantage of wet layup is that it is not easy to control the volume of resin put in the mould. Therefore, the part usually ends up being heavier than necessary because of low fibre content and consequently less strong.

Prepreg

A way to avoid the problems of wet layup is to use pre-impregnated fabrics, which allows controlling the volume of fibre in the part. The manufacturing process for prepregs is basically the same as for wet layup. It implies the use of an open mould and a vacuum bag (See figure 2.9). Placing the mould under vacuum in an autoclave (pressurized oven) during the cure increases the part quality. This process produces excellent parts and is widely used in aerospace industries. The problem with prepregs is that they are sometimes difficult to conform to complicated shapes. They also have to be kept in a freezer. Manufacturing composites parts with prepregs is essentially a manual procedure. However, some steps can be automated to increase process reliability and reduce labour. The rolls of material need to be cut to specific patterns to fit in the mould. This step can be done by hand with scissors and blades or with a computer controlled cutting table. After the patterns are placed and aligned in the mould, infrared beams can be used to indicate the contour of the location where the pattern should sit [16].

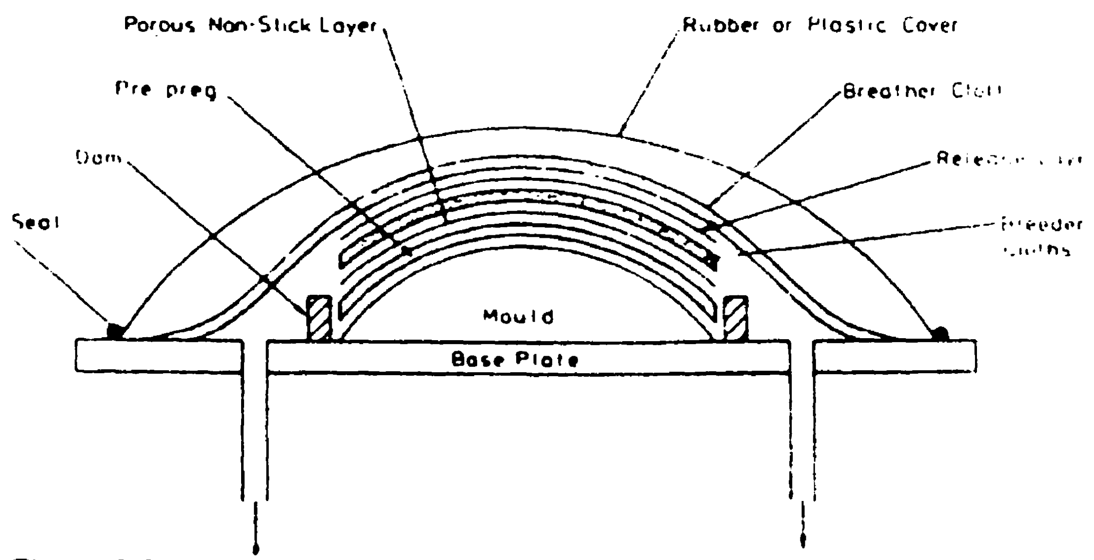

Figure 2.9: Vacuum Bag Technique [14].

Infusion

Infusion consists of placing dry fibre cloth (mat, unidirectional or woven) into an open mould and sealing the mould with a vacuum bag. The epoxy resin is then mixed with the hardener in a container. The container is connected to the mould with a tube and placed above the mould. The epoxy will then impregnate the fibres by gravity. A vacuum can be pulled to accelerate the process and increase the quality of the part. The vacuum bag is not rigid and can allow deformation easily while the mould is been filled. Therefore, it is very difficult to control the thickness of the part and the fibre content. Like wet layup, infusion yields parts with inferior material properties and is not suited for high performance composites.

Resin Transfer Moulding (RTM)

Resin transfer moulding consists of injecting liquid resin into a closed mould to saturate a reinforcement preform (See figure 2.10). The preform is the dry fibre arrangement of the composite part. The mould is generally made of metal and is machined to the outer shape of the part. This controls the thickness of the part at any location to a tight tolerance. Advantages for using RTM are: [17]

- Parts with high fibre volume (up to 70%)
- Repeatability of the process
- Part consistency
- Complex preform can be used

However RTM also has some disadvantages:

- Resin flow rate decreases as fibre volume increases.
- High fibre volume requires more time and energy.
- Resin tends to flow along fibre direction leaving dry spots.
- Complex preforms are more difficult to inject.

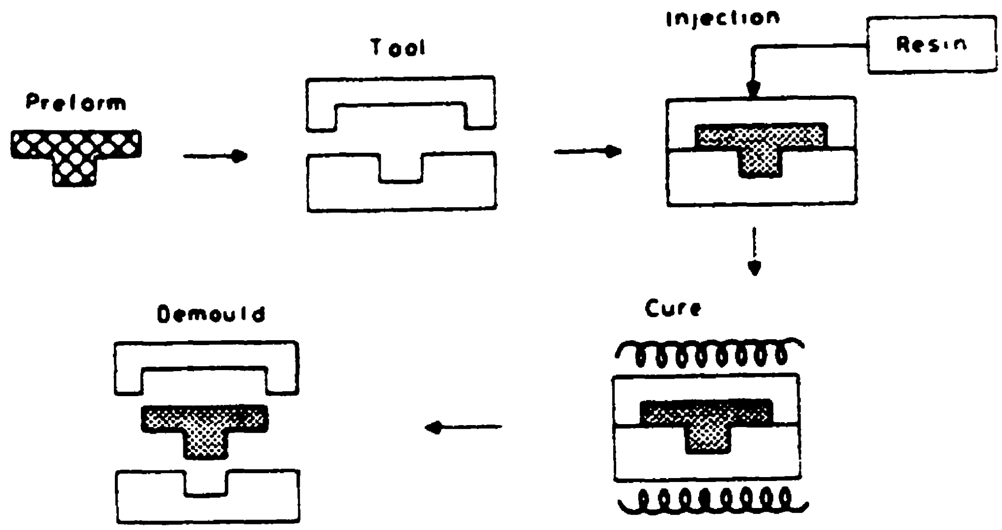

Figure 2.10: RTM Process Diagram [14]

The resin flow can be helped by pulling a vacuum in the mould prior to the injection. The commercial name for this process is VARTM (Vacuum Assisted Resin Transfer Moulding). It further reduces the possibility of voids and air bubbles trapped in the resin, therefore, increasing the overall quality of the part and optimizing the RTM process. And finally, the RTM process can be automated with a computer to control the resin flow and the injection pressure [18]. Also, simulation software has been developed at the École Polytechnique de Montréal to predict the progress of the resin flow front in the mould [19-23].

2.4 Composite Fork Review

Many composite forks can be found on the market. Different manufacturing methods are used, some that take great advantage of the composite properties and some that use composite material more for marketing than performance. The forks listed in Table 2.1 are high performance racing forks. Pictures of some of the forks are shown in figure 2.12.

Company	Model	Body Composition	Steerer	Length	Weight
Alpha Q	Standard	One piece carbon	Carbon	260mm	360 g
Alpha Q	Straigth blade	One piece carbon	Titanium	260mm	440 g
Columbus	Muscle	One piece carbon	Carbon	300mm	370 g
Columbus	Carve	Aluminium Crown with Carbon Blades	Aluminium	300mm	500 g
Kestrel	EMS road Ti	One piece carbon	Titanium	250mm	400 g
Kinesis	Saber	One piece carbon	Carbon	N/A	325g
Kinesis	Wedge	Aluminium Crown with Carbon Blades	Cromoly	N/A	530g
Kinesis	Carbon 2	Aluminium Crown with Carbon Blades	Cromoly	N/A	570g
Kinesis	Carbon 3	Aluminium Crown with Carbon Blades	Cromoly	N/A	570g
Kinesis	Airfoil	Aluminium Crown with Carbon Blades	Cromoly	N/A	640g
Profile Design	SC	Aluminium Crown with Carbon Blades	Aluminium	300mm	508 g
Profile Design	BDC	Aluminium Crown with Carbon Blades	Carbon	300mm	581 g
Profile Design	ACD	One piece carbon	Carbon	N/A	N/A
Profile Design	AC	One piece carbon	Carbon	300mm	345 g
Profile Design	BRC	Aluminium Crown with Carbon Blades	Carbon	300mm	504 g
Profile Design	BSC	Aluminium Crown with Carbon Blades	Aluminium	300mm	472 g
Reynolds	Ouzo Pro	One piece carbon	Carbon/Glass	285mm	375g
Reynolds	Ouzo Pro Aero	One piece carbon	Carbon/Glass	285mm	399g
Reynolds	Ouzo Comp	Aluminium Crown with Carbon Blades	Aluminium	285mm	500g
Serotta	F1	One piece carbon	Cromoly	350mm	700g
Wound Up	Road Fork	Aluminium Crown with Carbon Blades	Carbon	200mm	470 g
Wound Up	Cross Fork	Aluminium Crown with Carbon Blades	Carbon	200mm	545 g

Table 2.1: Different carbon fork available on the market [1] [24-29].

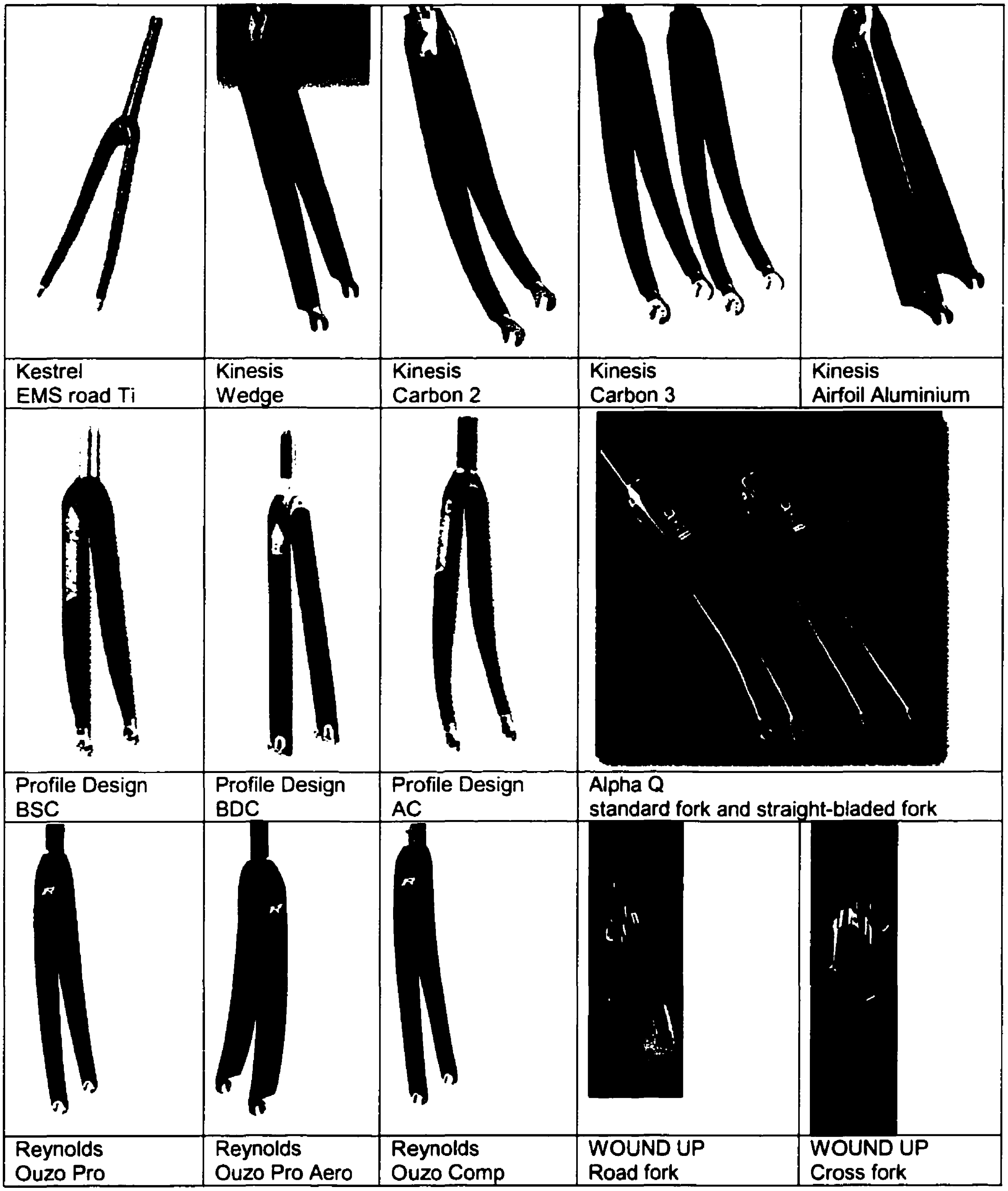

Figure 2.12: Pictures of Different Carbon Forks Available on the Market [24-29]

Chapter 3: Previous Fork Design and Analysis

3.1 Serotta F1 Carbon Fibre Fork

Figure 3.1: Picture of Serotta F1 Carbon Fork

This study is based on the original Serotta Carbon F1™ fork [1]. The F1 has many advantages, but one major problem in order to be competitive in the bicycle market. The F1 fork weighs twice as much as its competitors. However, the ride quality of the fork is incomparable and many consumers still want to ride it. Sooner or later, the drawback of its weight will greatly reduce its popularity and sales.

Over the years, the F1 fork has proven itself to be dynamically stable even at high speed and when cornering. It has also shown excellent fatigue durability. In tests, the F1 fork surpasses many forks, even all-metal forks. This makes the F1 very reliable especially since its mode of failure is not catastrophic. The ride quality and the long life of the fork should not be compromised in the redesign of a lighter version.

The Serotta F1 fork is a rigid road fork that fits a wheel of 700 cm of circonference, commonly called a 700cc wheel, and has a rake of 43mm (See figure 2.3). The fork is made by RTM in a closed mould. The composite structure consists of carbon fibre braids over a high-density foam core and is injected with a thermosetting epoxy resin. The Serotta F1 fork is composed of a steel assembly steerer insert (See figure 3.2), carbon legs and two titanium dropout inserts (See figure 3.4). Final machining and finishing is required when the fork is removed from the mould. The crown race seat needs to be machined to a tight tolerance for press fitting the bearing race. The ends of the legs are bored afterward and the dropouts are bonded in the bored holes.

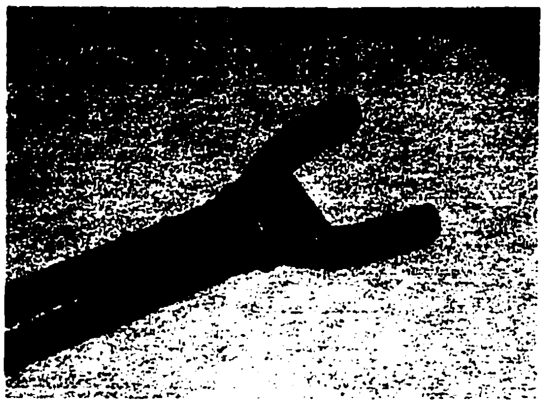

Figure 3.2: Picture of the F1 Fork Steerer.Tube Insert

The steerer assembly consists of a steerer tube, a crown race ring and two small legs, all welded together. The small steel legs provide a transition between the steerer tube and the carbon blades. The steel is composed of chromium-molybdenum, a common alloy used in the bicycle industry and referred to as "Chrome-Moly".

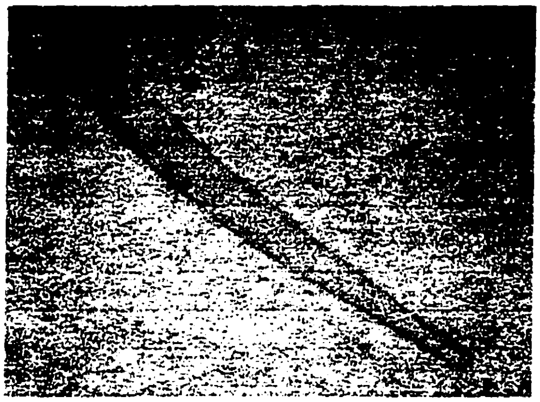

Figure 3.3: Picture of F1 Fork Foam Core

The foam core is made out of high-density polyurethane foam. The foam comes in sheets and it is machined to the perfect shape to allow a good ratio of fibre versus resin (Explained in section 5.4.)

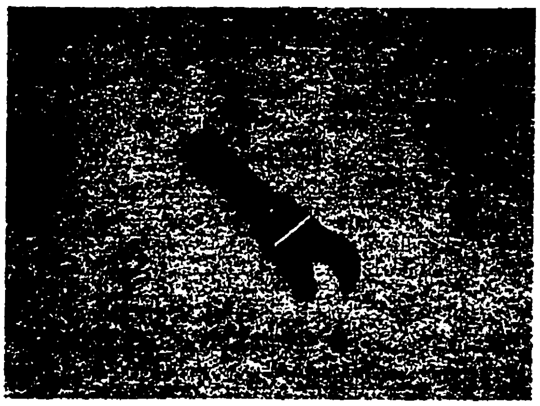

Figure 3.4: Picture of F1 Dropout Insert

The dropouts are machined from a solid piece of titanium. After the full cure of the fork, the ends of the legs are cut and bored for bonding the dropouts. A high strength adhesive epoxy is used to fix the dropouts to the fork.

Two grooves are machined in the shaft of the dropouts. The grooves are filled with epoxy during the bonding process. The epoxy pockets help prevent the dropouts from coming off the fork in the event of bond failure [1].

3.2 Finite Element Analysis

This is the summary of a previous finite element analysis of a carbon fibre fork by Todd Turner [30]. The fork is the Serotta F-1 Carbon Fibre Epoxy Composite Fork Model.

3.2.1 Meshing

The meshing was divided for each kind of part in order to use the appropriate material properties. Moreover, different kinds of elements were used to model the fork, as accurately as possible. Thus, 2D and 3D elements were used.

Steerer tube	Lower part: solid elements Upper part: shell elements
Crown	Solid elements
Blades	Shell elements
Dropouts	Solid elements

Table 3.1: Meshing description

3.2.2 Loading and Boundary Conditions

The top and the base of the steerer tube are clamped. The dropouts are restrained in the x-direction. The loading is a lateral load of 2000 N. Four nodal points on each dropout are used to apply a load of 250 N, for a total of 1000 N applied to each blade. The direction of the force is along the negative Z-axis (See figure 3.5).

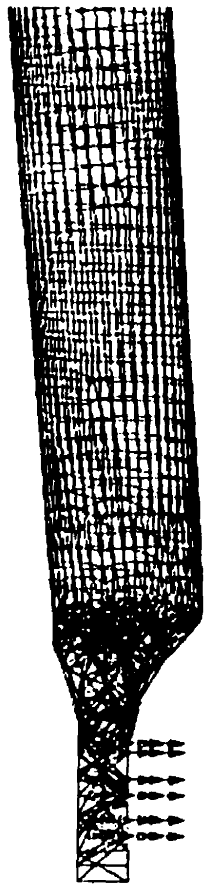

(a). Front View

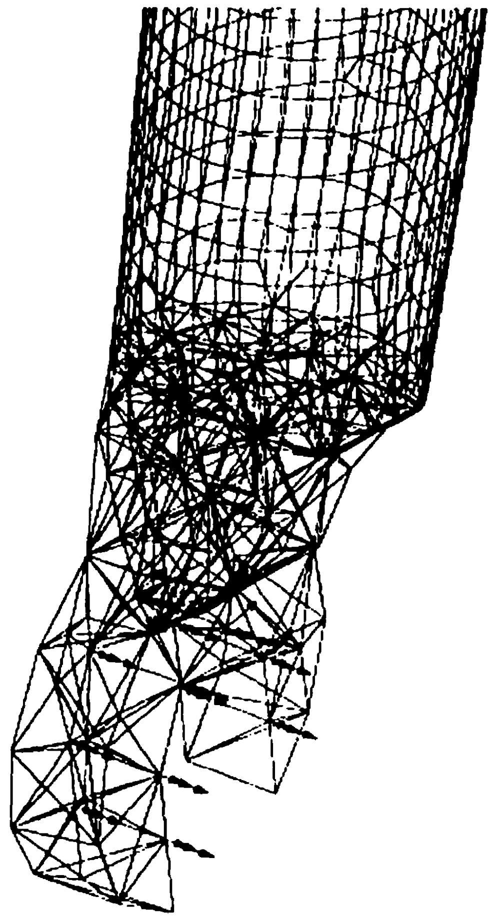

(b). Front Isometric View

Figure 3.5: Dropout Load Application Boundary Condition

3.2.3 Results

Steerer Tube

No stress concentration, except for the few small regions along the connection with the lower half of the steel insert. These few small regions of elevated stress are a result of the connection between the shell elements of the steerer tube and the solid elements of the insert. [30]

The highest stresses are found near the hole, with the largest value being 93.4 MPa as the maximum principal stress component. This is approximatively 30 % of the yield stress, and therefore the insert should exhibit no sign of plastic deformation. [30]

Epoxy Layer

Two high stress regions are apparent and these areas have stresses, which are high enough to cause failure in the epoxy. The first region occurs at the bottom of the arm of the insert, and is seen to have stresses as high as 38.10 MPa in the maximal principal stress component and 46.0 MPa in the Von Mises component. [30]

Failure also occurs in a second region along the top lip of the epoxy layer, and has a similar stress value as the first region. [30]

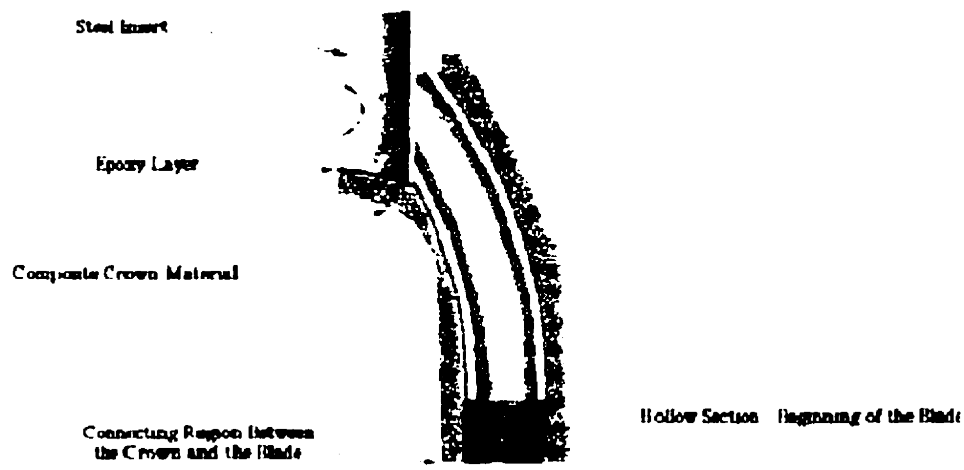

(a). Half-Plane of the Crown Region

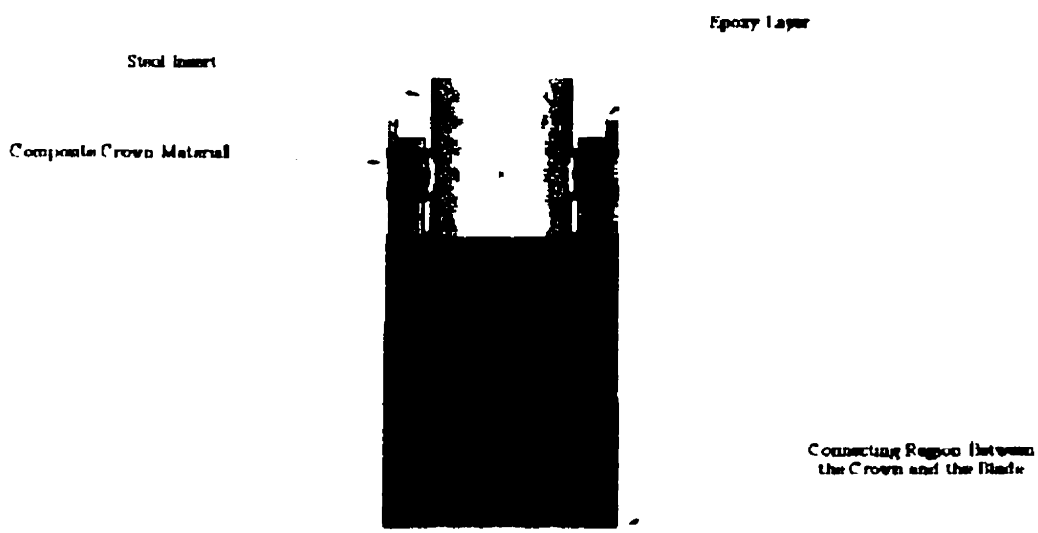

(b). Midplane of the Crown Region

Figure 3.6: Two Different Cross Sections of the Solid Geometry in the Crown Region

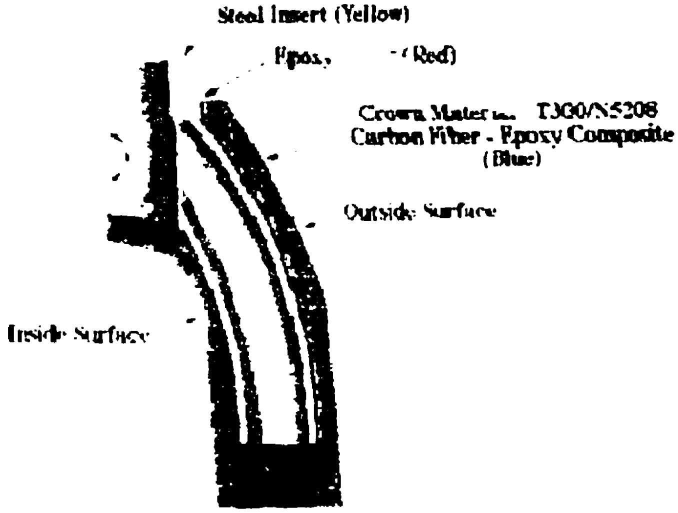

(a). Solid Geometry - Half Plane of the Crown Region

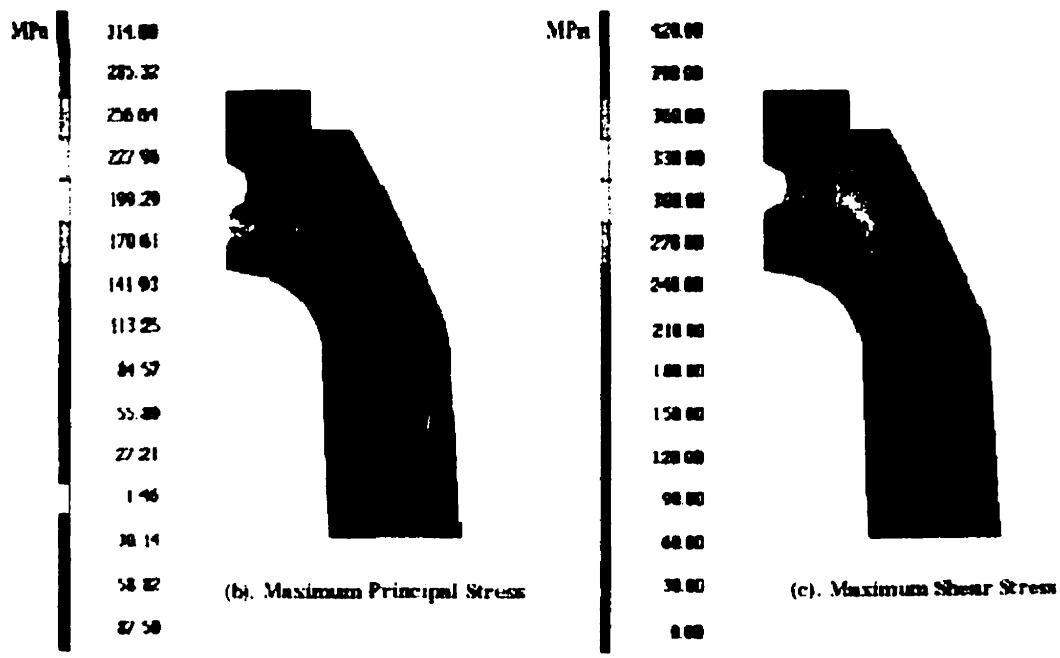

(b). Maximum Principal Stress

(c). Maximum Shear Stress

Figure 3.7: Midplane of the Crown Region

3.3 Summary of Test Results

Finite element analysis was very useful in determining the problematic region where failure could occur. The specific analysis of the steel insert and of the carbon fibre blades demonstrates that the stress levels in those regions were below the yield strength of the corresponding material (steel or composite). However, high stresses were found at the interface between the steel insert and the carbon-epoxy composite that could cause failure. Experimental fatigue tests showed that failure occurred in this region.

Chapter 4: New Carbon Fork

The main goal of this project is to develop a lighter version of the Serotta F1 fork while keeping the same philosophy behind the product. The philosophy to be respected in the fork redesign consists of the following: "Classical" shape, lightweight, durable, with an optimum ride quality.

Designing a composite part is a multidisciplinary task. The design of the part has to progress simultaneously in several different aspects: CAD, Composite Structure, Insert Design, Composite Manufacturing Method, Finishing and Final Machining of the part. No areas of design can be completed before the others are defined since they all influence each other.

4.1 Computer Aided Design (CAD)

The first criterion to respect in the design is the external shape of the fork. The current Serotta F1 fork is of a "Classical style" and is compatible with most road frames on the market. The style lines are not to be modified extensively and it is on these lines that the design process begins. The lines consist of a blend from an elliptical cross section of the upper region of the leg to a round cross section down at the drop out. The majority of the design effort will concentrate on the internal composition of the fork: composite structure and insert design.

The fork dimensions are based on commercially popular designs. The span of the fork will accommodate 700cc wheel geometry with enough clearance at the shoulder area for a 28mm tire width. The rake of the fork will be 55mm to provide a comfortable ride while still being responsive. The fork body is designed for a 1" diameter steerer tube. This dimension is still the industry standard but should soon be replaced by the new standard of 1.125" derived from the mountain bike industry.

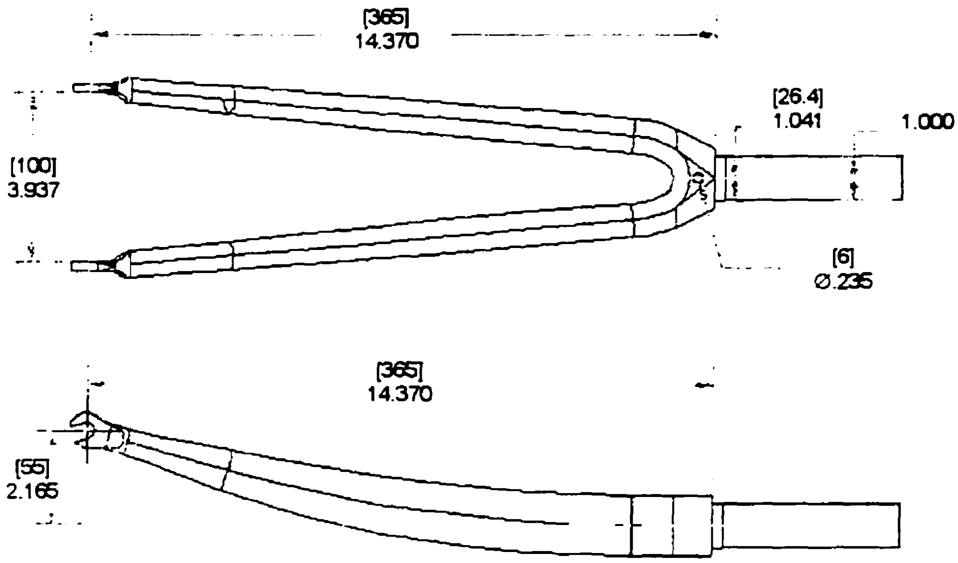

Figure 4.1: Fork Dimensions for the New Design

4.2 Composite Structure

A quick analysis of the current F1 fork reveals that half its weight is due to the steel insert. Also, from the finite element analysis and the experimental mode of failure, it shows that the crown race is the critical area of the fork [30]. The redesign will therefore concentrate on modifying or replacing the entire steel insert.

Before redesigning the fork one must look at the function of the fork:

- Support the front wheel
- Provide lateral support for control
- Provide vertical support
- Provide vertical compliance for comfort
- Attach to bicycle frame
- Provide steering
- Adjustment of steerer length for compatibility with different bicycle frames
- Compatibility with standard equipment (wheel axle, brake, stem and bearing)

All the steps of cutting the steerer tube to length, press fitting the bearing race and adjusting the bearing tension are made by bike mechanics in a store or directly by the customer. It is then very difficult for the fork manufacturer to control the quality of the fork installation and therefore great care should be placed in making those steps as easy as possible.

The tendency in the market is toward a threadless steerer design (See section 2.2). Therefore the new fork redesign will concentrate on making it primarily compatible with the threadless style head set.

The material options for building the fork and its inserts are aluminium, titanium, high-grade steel and carbon fibre composites. A strength-to-weight ratio analysis clearly shows a major advantage for carbon fibre. However the interaction of the fork with its surroundings shows some limitations to an all composite fork. A titanium insert has already been tried as a replacement for steel, but two problems arose. First, titanium tubing did not show the stiffness in the stem region required for the ride quality sought.

The first idea was to remove the steel insert completely and build a monocoque composite structure. This would allow for a great reduction in weight while keeping the performance optimal. However the ruggedness of the fork installation process might create a stress point in the fork and considerably reduce the strength of the fork. The hoop stresses produced by press fitting the bearing race can also cause premature failure. The placement of the star-flanged nut and the clamping of the stem could damage the steerer tube. It was then decided, for safety reasons, to have metallic interfaces on the fork for installing the surrounding components. The metallic inserts are then the dropouts and a steerer tube with a shoulder for the bearing race. The steerer tube does not need to be threaded since the redesign is oriented toward the threadless system.

4.3 Insert Design

4.3.1 Steerer Tube

The best solution found for the steerer tube is a hybrid metal/carbon fibre structure. The carbon fibre arrangement will provide sufficient stiffness for the performance of the fork while the metal will offer appropriate surfaces for the interfaces. Steel is very heavy and corrodes under natural weather conditions and should thus be avoided in lightweight structures. A phenomenon called galvanic corrosion occurs when graphite is in contact with metal. Indeed, graphite can act as a cathode when in contact with some metals and this can lead to deterioration of the metal [31]. Aluminium is prone to galvanic corrosion and should be electrically insulated for composite applications. However, titanium does not induce galvanic corrosion when in contact with graphite [34]. The metal of choice is then titanium since it offers the best compatibility with composites [31-34] and is fairly lightweight.

The steerer insert should go down in the crown to the brake hole (for drilling the brake hole) in the insert, but enough clearance is needed to allow a carbon/epoxy structure to go up inside the steerer tube for stiffness. Also a circumferential surface with a shoulder is needed for pressing and locating the bearing race. The top end of the steerer tube should be easy to cut to the desired length and offer a good internal surface for the star-flanged nut as well as a good external surface for clamping the stem.

The steerer tube insert is made of three parts: the steering column, the bearing race seat and the brake insert. The steering column and the bearing race seat are made separately in order to use stock material tubes and to minimize machining time and material waste. The steering column is cut to length. The bearing race seat is cut to length and the race seat shoulder is pre-machined. Both pieces are press fit together, and then they are drilled, mitered with a hole saw and chamfered to final shape.

The brake hole insert has a sliding fit with the steerer tube insert. The brake insert is assembled after the carbon fibre legs are placed inside the steering column. The purpose of this insert is to provide support for the brake bolt and to avoid crushing the composite structure when tightening the bolt. It also serves as a safety pin in case the carbon legs and the steerer tube delaminate.

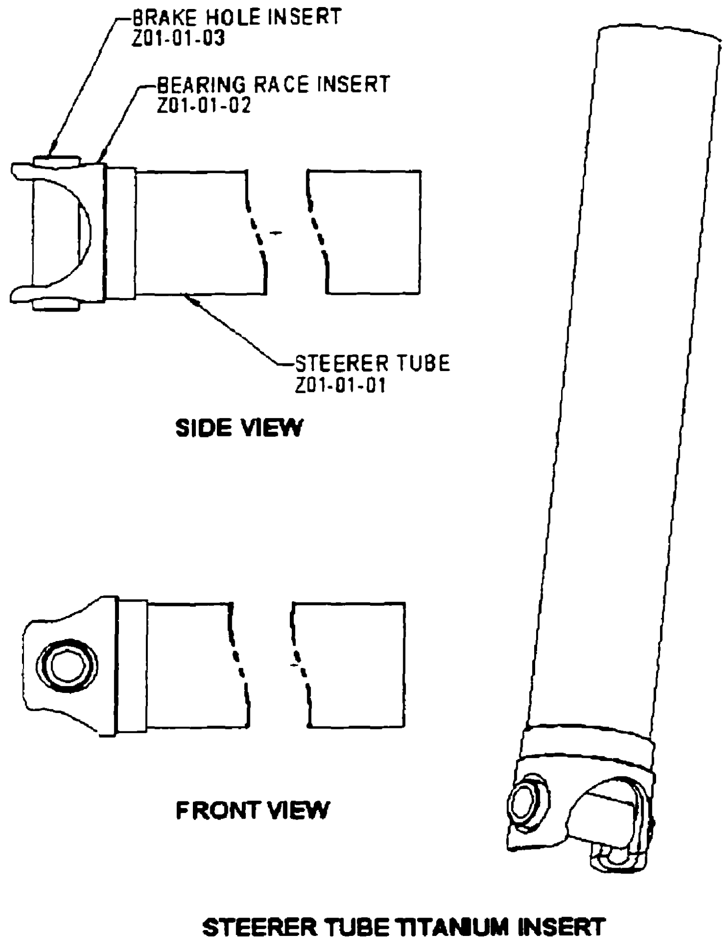

Figure 4.2: Steerer Tube Insert

4.3.2 Dropouts

The dropouts used for the old F1 fork work perfectly and do not need to be redesigned. However the dropouts were redesigned for manufacturing. The overall shape did not change but the way the dropout is machined is now different and more efficient. The dropout is now machined from a 7/8" (22.2 mm) diameter solid rod of titanium. The first machining step is on a computer-controlled lathe that turns the contour. The turned piece is then transferred in a computer-controlled milling machine to give the final shape.

4.4 Finite Element Analysis (FEA)

A finite element analysis (FEA) was performed in order to study ways for improving the new structure behaviour. The analysis was started at the beginning of the study and choices for material and specific ply arrangement were made from general composite material properties regardless of the manufacturing process under development. Those properties would later help define which fibre/epoxy combination to choose from the ones available on the market.

The general design concept is to keep the same carbon blade design as the F1 fork and replace most of the steel insert with equivalent carbon reinforcement layers. With composites showing strong anisotropic behaviour, it is difficult to exactly translate the steel insert properties into a carbon structure especially in an area where different stresses flow through the material.

At the same time, a ply composition has to be defined to start the analysis. The nature of the fork loading consists mostly of a downward force from the rider's weight, compressive loads and some moments from road bumps (the fork steerer axis is at a 73° angle from the ground) and finally torsion and lateral forces from turning. The type of loads the forks undergo inspires the fibre arrangement. Most of the fibres should be unidirectional because of the compressive forces and moments from weight and bumps, and because of lateral forces. Finally, ±45° fibre layers are needed for torsional stiffness and overall stability.

4.4.1 Load Cases and Boundary Conditions

The load cases [35-37] were developed from previous finite element and experimental analysis. Two different directions of loading were judged adequate to determine basic fork behaviour. The first load case corresponds to a frontal impact. The common head tube angle for a bicycle frame is 73°; therefore, the load applied at the dropouts is at a 73° angle from the steerer tube axis. The data collected form this case is a dropout displacement from which a fork frontal stiffness is calculated and compared with experimental results.

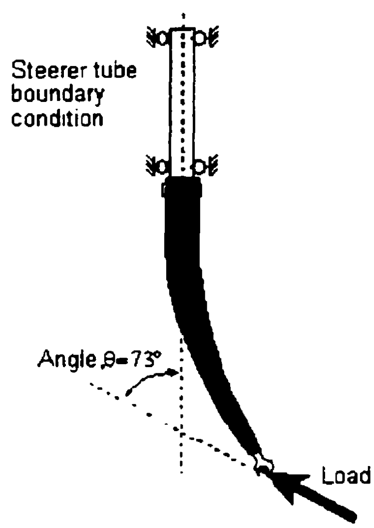

Figure 4.4: Front Stiffness Test Diagram

The second load case consists of applying a transverse load at the dropouts. This load case represents part of the load a fork undergoes when the bicycle and rider are taking a turn. This setup measures a displacement at the dropouts that is interpreted as a lateral stiffness and also used for experimental comparison.

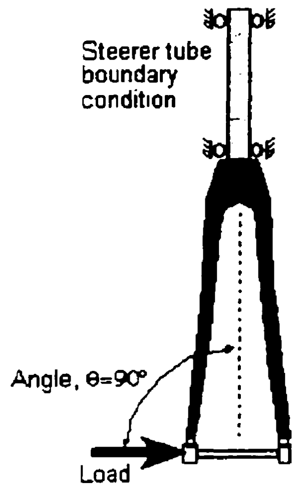

Figure 4.5: Lateral Stiffness Test Diagram

In both cases, the boundary conditions try to simulate the headset in which a fork is typically mounted. The headset is a combination of two bearings where the fork is held in place with a retaining nut and a tensioning screw. The first bearing is mounted directly at the fork shoulder and the second one is at the top of the steerer tube where the stem is attached. The corresponding boundary condition is one with all translation degrees of freedom (XYZ) fixed and with all rotation degrees of freedom free.

4.4.2 Software Computation for the Finite Element Analysis

A static finite element analysis has been performed with the software I-DEAS to confirm the design, to choose the composite lay-up and to predict the failure point revealed with the fatigue test. This analysis shows the displacements and stress concentrations for the two loading configurations mentioned above with increasing loads. Particular attention has been given to stress concentration areas. The static behaviour will be analyzed and compared to experimental fatigue results.

4.4.3 Meshing Definition

As the fork is composed of different materials (carbon fibre lay-up and titanium) in different layers, the model had to be a 3-D model. The main effort has been made on the meshing to guarantee accurate results. Thus, orthotropic cubic elements were used as much as possible.

The best way to create proper cubic meshing is to use an option called "Mapped Meshing". The "Mapped" meshing option allows controlling the placement, quality and density of created elements. In order to mesh the different parts of the fork with cubic elements, solid partitions were used with mapped meshing as shown in figure 4.6.

However, intricate parts are not possible to mesh with the mapping option. The geometry of the fork crown prevented correct partitions for mapped meshing. The crown was therefore meshed with tetrahedral elements with the free mesh option controlled by an internal algorithm. The steerer, in contact with the crown, also had to be meshed using tetrahedral elements.

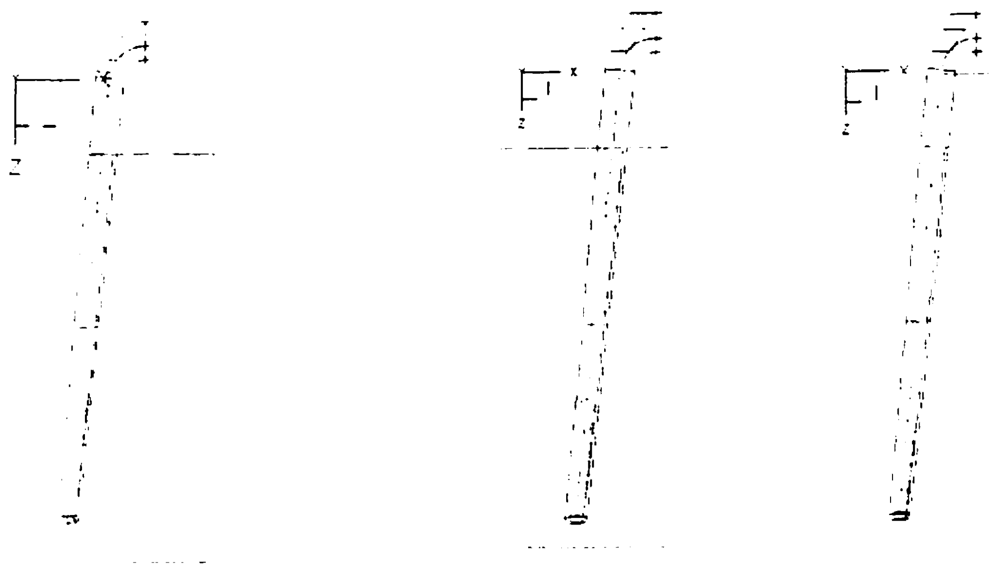

(a) Partition 1 (b) Partition 2 (c) Partition 3

Figure 4.6: Fork Partitions Used for the Meshing

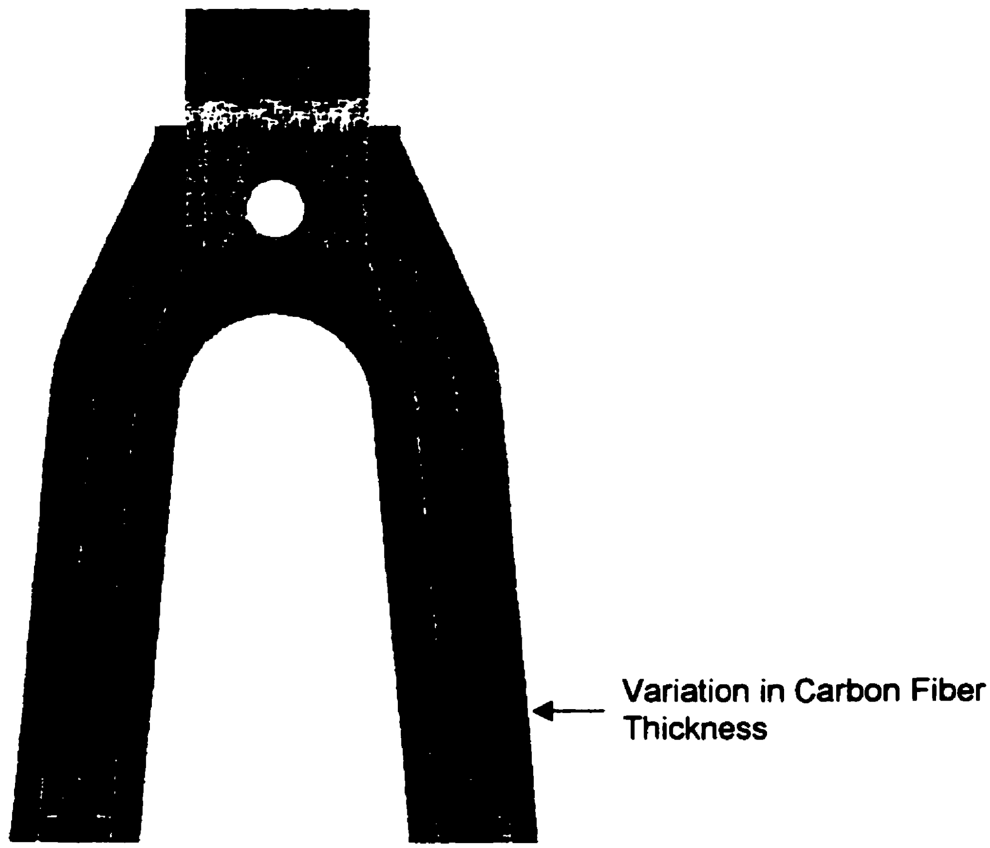

Figure 4.7: Meshing Magnification Around the Crown

Figure 4.7 shows the final meshing of the fork with the two blades using cubic elements and the crown and steerer using tetrahedral elements.

4.4.4 Material Properties

The carbon layup of the fork is composed of two different ply arrangements. The first zone is made of 4 layers located in the blades below the crown region. The second zone begins at the bottom of the crown region and goes up in the steerer tube. The variation in the layers can be seen in figure 4.7. The upper zone has twice the layers as the lower zone to replace the steel insert used in the F1 fork. The second material used in the model is titanium for the steerer tube insert.

The material used for the analysis is a general use prepreg material from "The Advanced Composites Group" [38]. Both the unidirectional plies and the woven material use a LTM 25 resin system [38]. The layer distribution for the first zone is one layer of woven at $\pm 45^{\circ}$, two layers of unidirectional at 0° and one layer at $\pm 45^{\circ}$. The second zone has the same four layers starting from the external surface followed by another layer of $\pm 45^{\circ}$ and three more unidirectional layers at 0°.

For this study, the mechanical properties have been calculated with a specialized software, called MLAM, developed at McGill University [39]. MLAM uses the previous equations to calculate the overall material property values. The advantage of using the software is that different ply configurations can be simulated rapidly. The values kept in table 4.1 were judged to be adequate for this study.

Property and symbol	Units	Zone 1	Zone 2
Fiber Direction Modulus Ex	GPa	59.47	25.73
Matrix Direction Modulus Ey	GPa	20.9	16.99
Out of Plane Modulus Ez	GPa	20.9	16.99
Gxy	GPa	11.8	14.166
Gyz	GPa	19.67	23.61
Gxz	GPa	19.67	23.61
Poisson's Ratio ν_{xy}	-	0.26	0.43
Poisson's Ratio ν_{xz}	-	0.26	0.43
Poisson's Ratio ν_{yz}	-	0.3	0.3

Table 4.1: Properties of Composite Materials.

4.4.5 Loading and Boundary Conditions

As shown in figure 4.8, the nodes of the two extremities of the titanium steerer were restrained in displacement with free rotation (ball joint) and the forces were applied on two nodes at the extremities of the two blades.

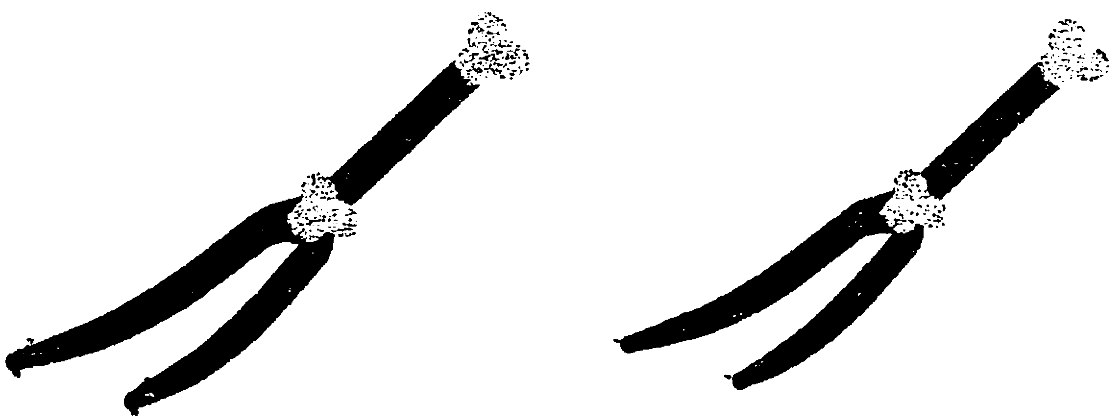

1st Loading Case and BCs 2nd Loading Case and BCs

Figure 4.8: Model First and Second Load Case With Boundary Conditions

4.4.6 Results and Conclusions

Inward Load

The static test results from the finite element analysis are shown in table 4.2.

Loading (N)	Von Mises Stress (Pa)	Maximum Principal Stress (Pa)	Displacement (mm)	Stiffness (N/mm)
1000	8.06E+05	9.60E+05	16.6	60.2

Table 4.2: Results Table for Inward Loads

As expected, we can notice in figure 4.10 that the maximum displacements occur at the extremities of the two blades. As the problem is symmetric, the two ends have the same displacements. The deformations in the steerer are negligible compared to the deformations in the two blades.

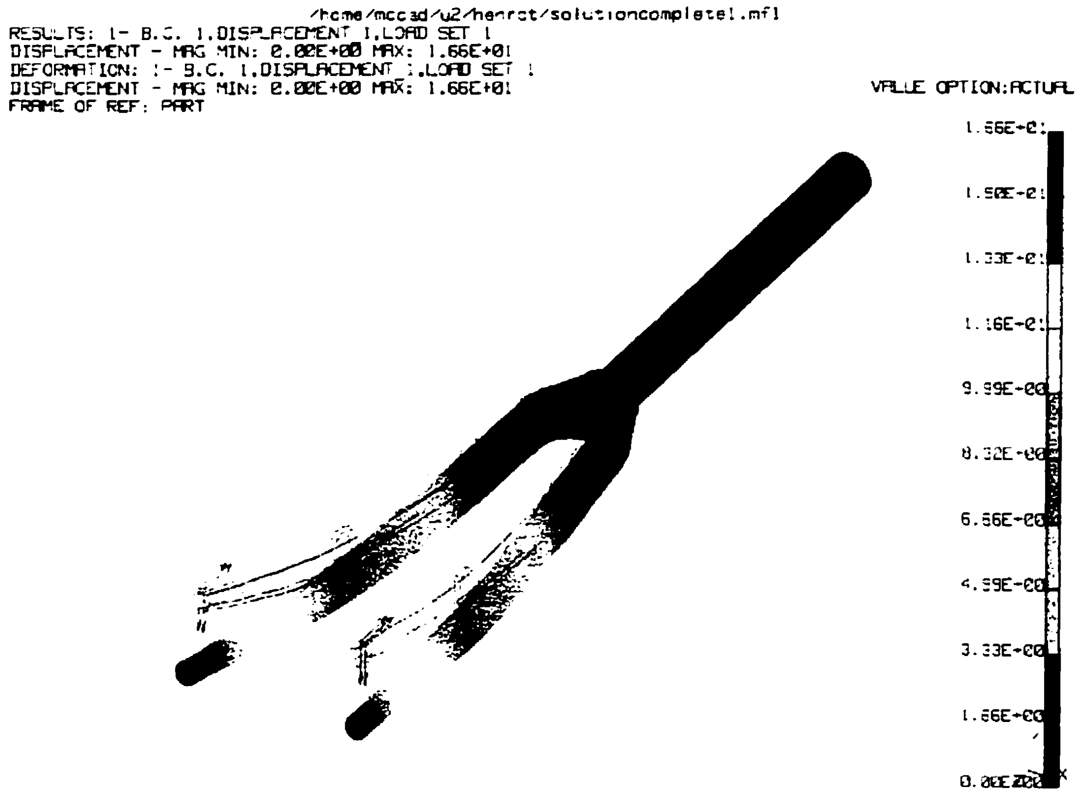

Figure 4.9: Displacement (Magnitude)

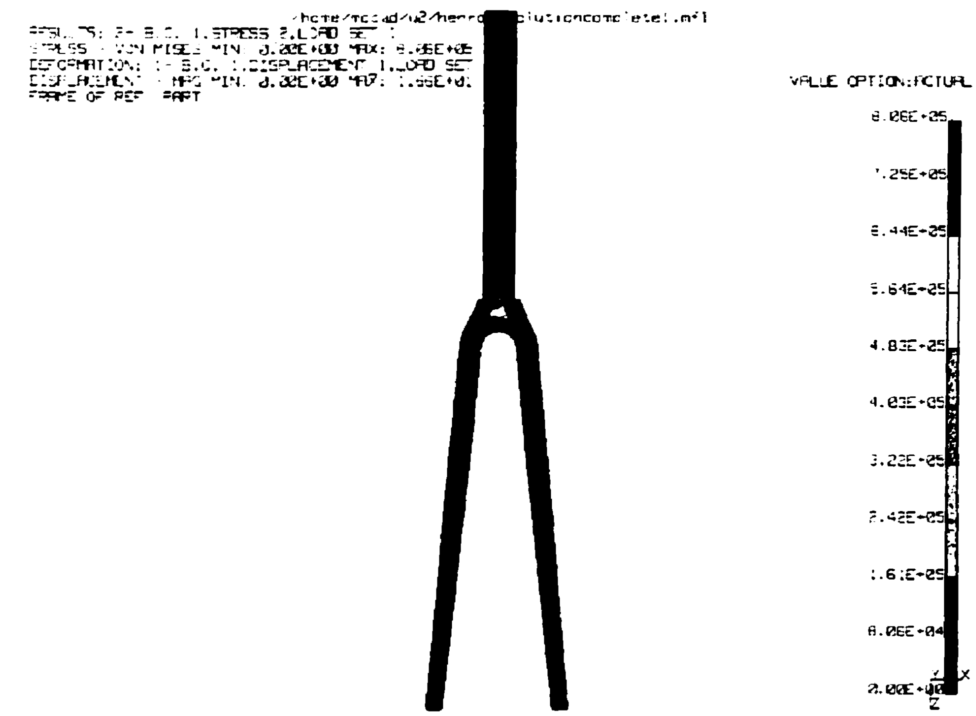

Figure 4.10: Front View Showing the Von Mises Stress Distribution

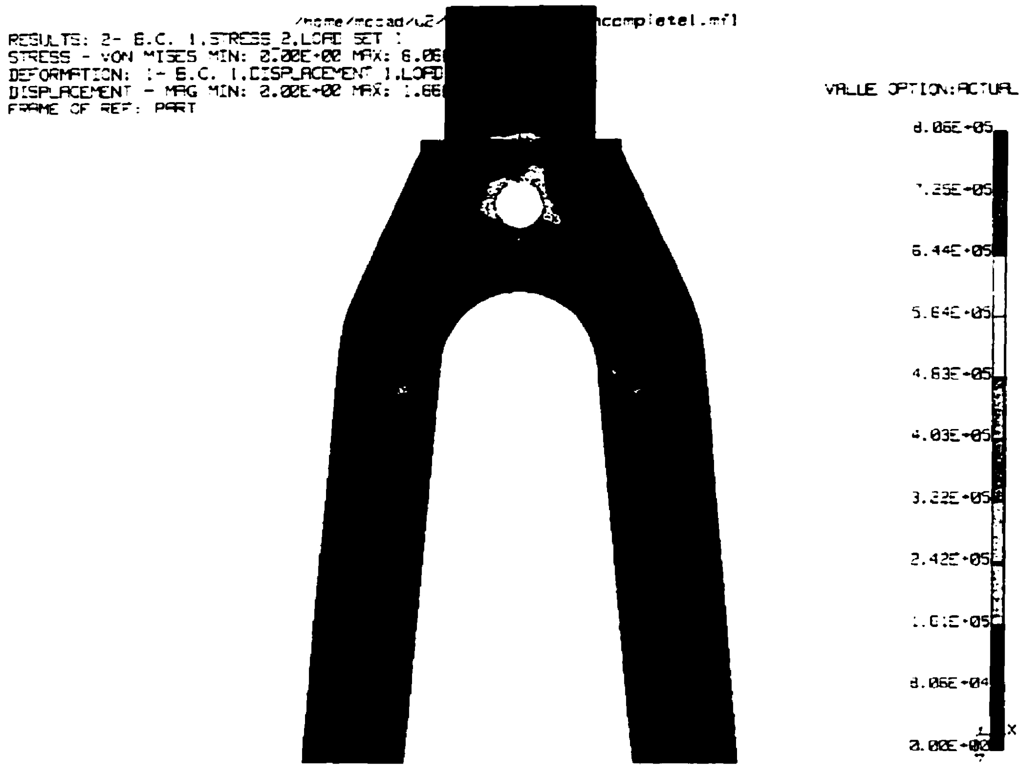

Figure 4.11: VM Stresses: Magnification of the Crown (Front View)

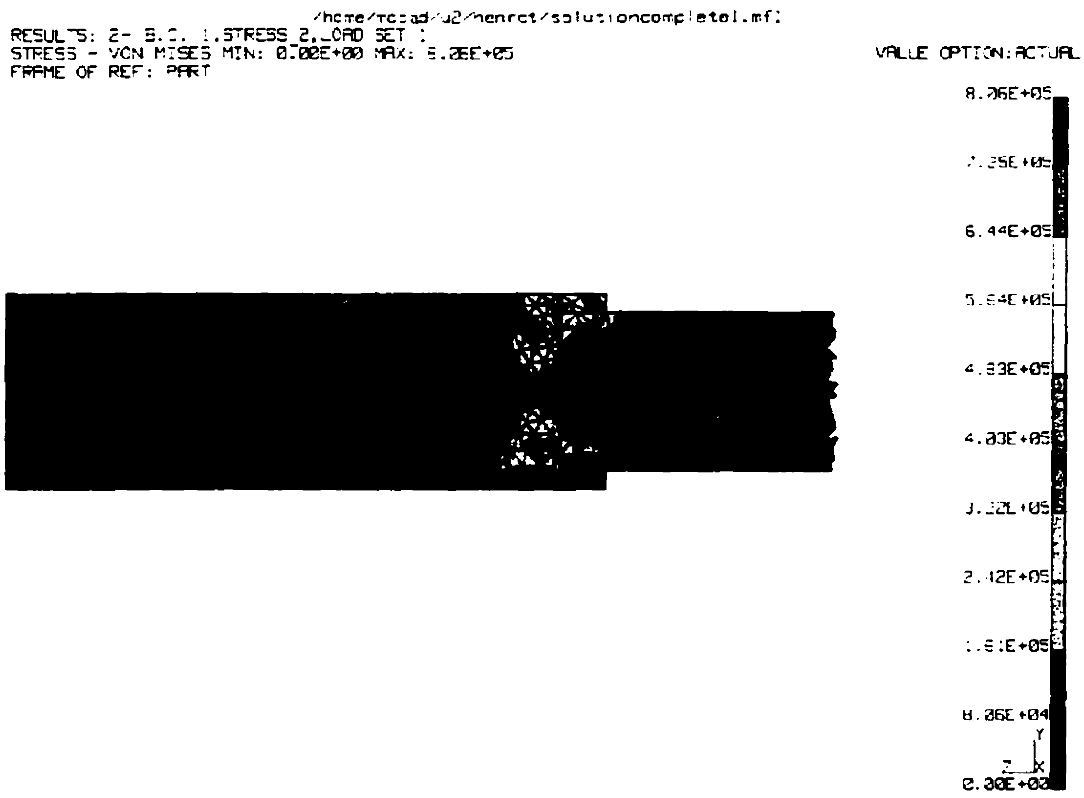

Figure 4.12: VM Stresses: Magnification of the Crown (Cut)

As shown on figures 4.10, 4.11 and 4.12, there is an expected accumulation of stress at the front line between cubic and tetrahedral elements. But the most critical stress accumulation is around the hole (top and bottom of the hole). This could induce failure or debonding between the steerer and the composite when the fork is highly loaded or tested in fatigue.

Lateral Load

Table 4.3 shows the maximum values of stress and displacement calculated at two different loadings.

Loading (N)	Von Mises Stress (Pa)	Maximum Principal Stress (Pa)	Displacement (mm)	Stiffness (N/mm)
500	2.46E+05	4.39E+05	19.6	25.51

Table 4.3: Maximum Values for Lateral Load

As expected, we can notice in figure 4.15 that the maximum displacements occur again at the extremities of the two blades. This time, even though the loading is not symmetric, the two ends have however the same displacements.

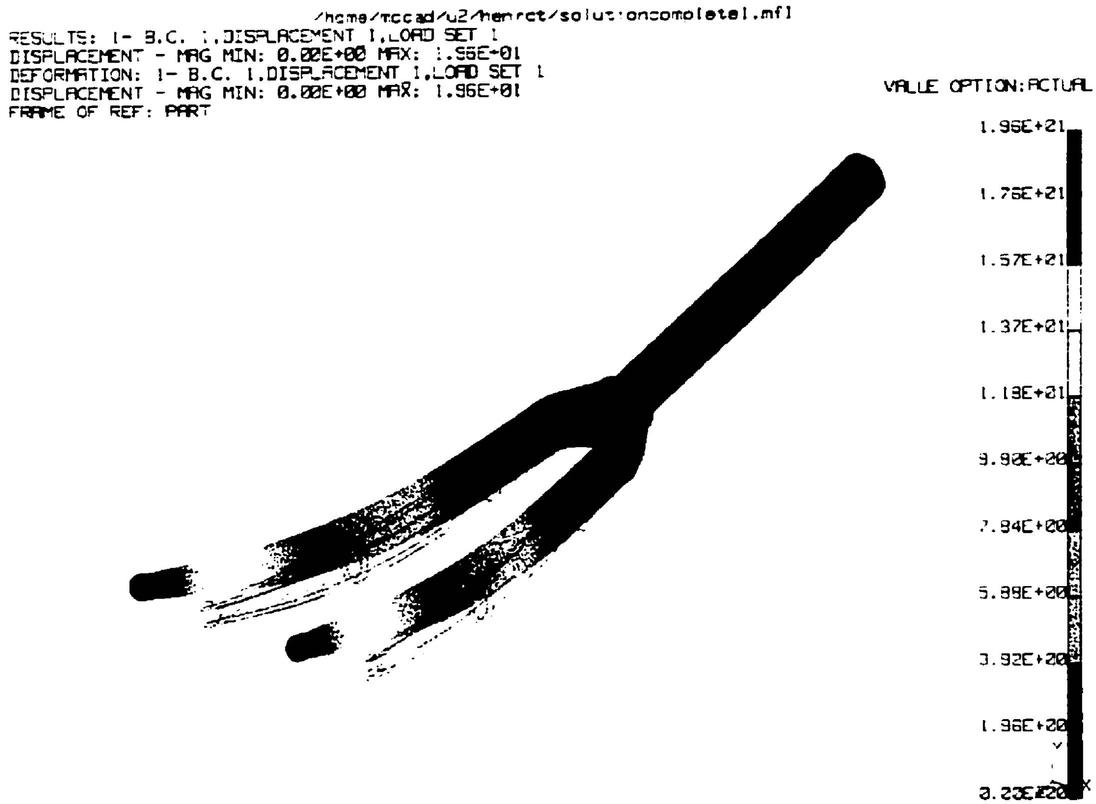

Figure 4.13: Displacement (Magnitude)

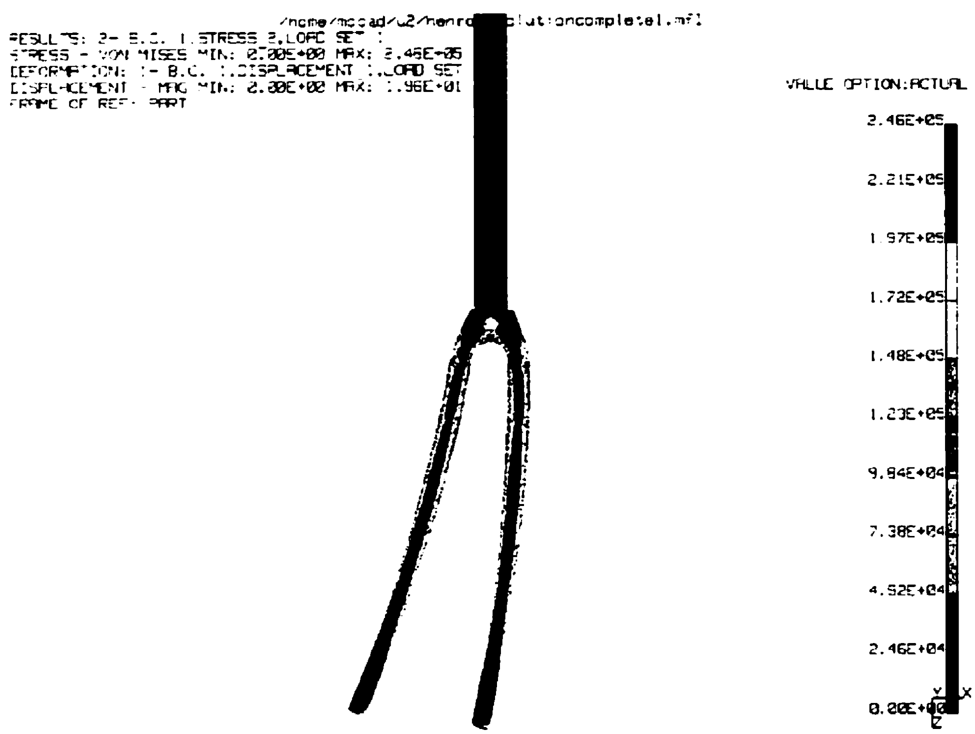

Figure 4.14: VM Stresses: Front View

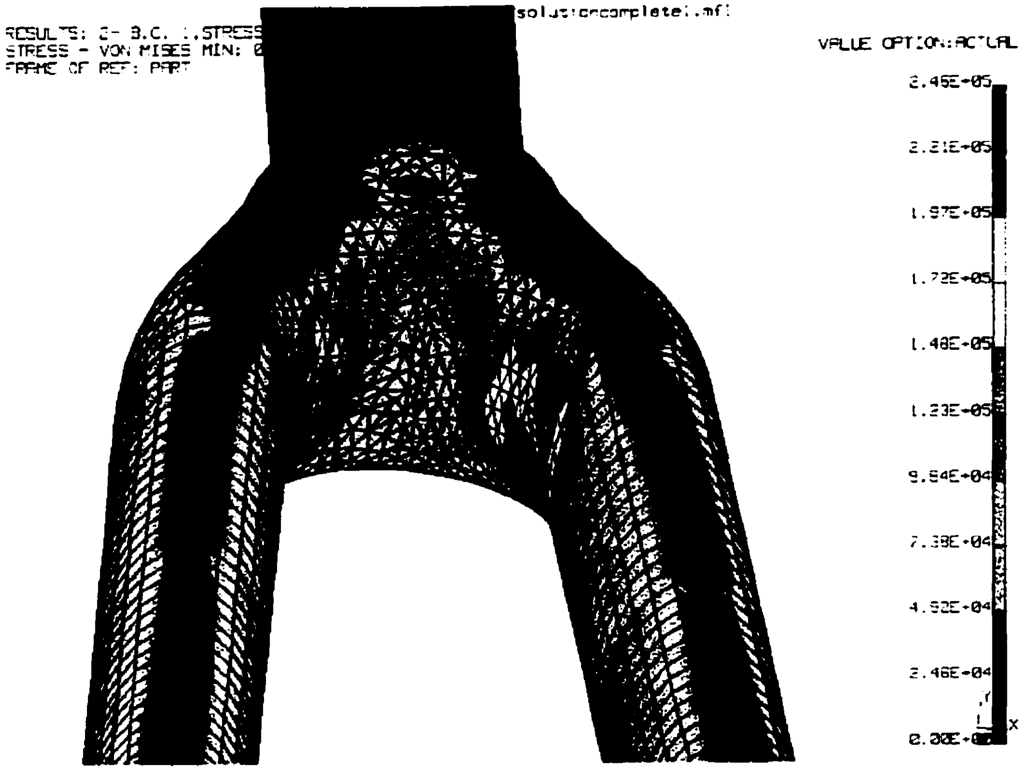

Figure 4.15: VM Stresses: Magnification of the Crown (Front View)

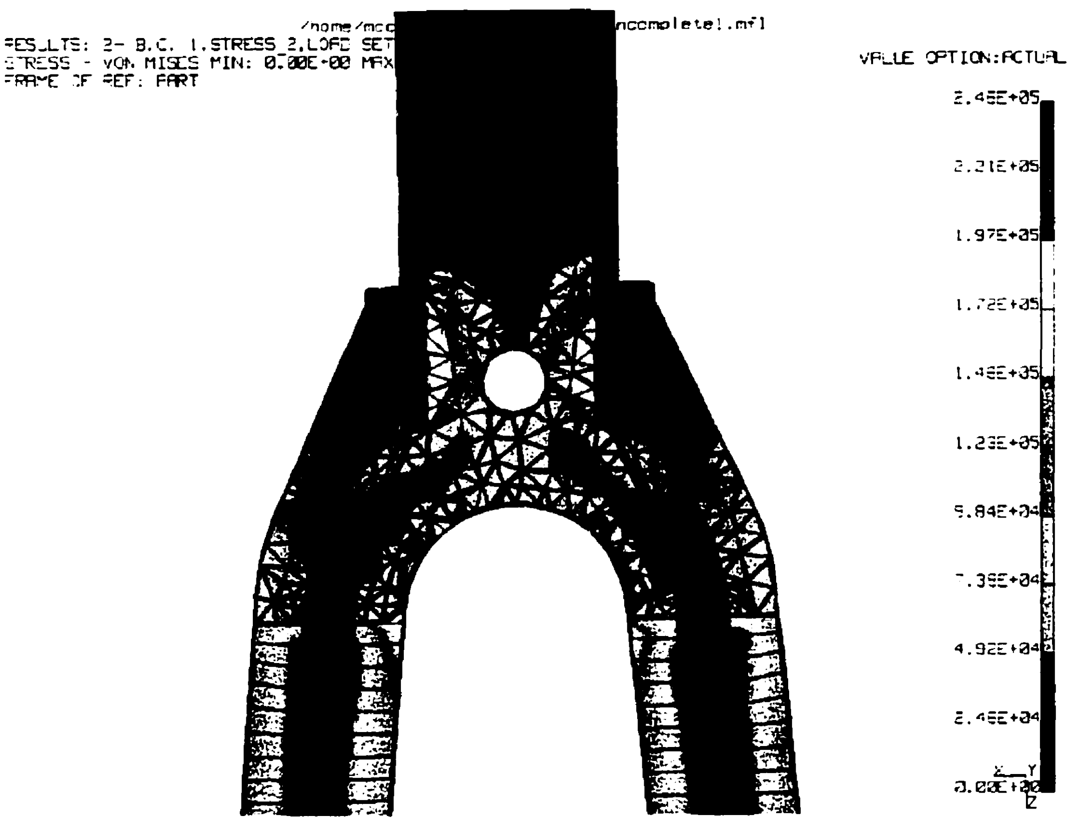

Figure 4.16: VM Stresses: Magnification of the Crown (Cut)

As shown in figures 4.14, 4.15 and 4.16, there is again an expected accumulation of stress at the front line between cubic and tetrahedral elements. The external layers are regions of high stresses but the most interesting region is the stress accumulation in the composite inside the steerer. This could again induce failure or debonding between the steerer and the composite when the fork is high-loaded or tested in fatigue.

From the finite element analysis, several approximations made the results unreliable.

- The volume ratio of fiber over resin cannot be practically constant everywhere.
- The principal orientation of the fibers is not always along the z axis.
- The Poisson ratio is not correct for the 8-layer lay up.

Table 4.4 and 4.5 show a summary of the FEA analysis.

Part	Regions	VM stress for 1000N Loading (MPa)	Comments
Steerer Tube	• Lower part on the sides of the brake hole	1.5 E5 < stress <8.1E5	• Critical region for failure and debonding
	• Rest of the tube	0 < stress <2.5E5	• No critical stress
Crown	• Around the brake hole	2.5 E5 < stress <8.1E5	• Critical region for failure and debonding
	• Interface with steerer tube	2.5 E5 < stress <8.1E5	• Critical region for failure and debonding
	• Rest of the crown	0 < stress <2.5E5	• No critical stress
Blades	• Along the blades (front and rear sides)	0 < stress <2.5E5	• No critical stress
	• Rest of the blades	nearly none	• No critical stress

Table 4.4: Summary of FEA Results for Frontal Loading

Part	Regions	VM stress for 500N Loading (MPa)	Comments
Steerer Tube	• Lower part on the sides	5E4 < stress <2.5E5	• Critical region for failure and debonding
	• Rest of the tube	0 < stress <5E4	• No critical stress
Crown	• Around the holes	5E4 < stress <2.5E5	• Critical region for failure and debonding
	• Bottom arch	5E4 < stress <2.5E5	• Critical region for failure and debonding
	• Interface with the steerer tube	5E4 < stress <2.5E5	• Critical region for failure and debonding
	• Rest of the crown	0 < stress <5E4	• No critical stress
Blades	• Along the blades (right and left sides)	0 < stress <1.5E5	• Critical region for failure and debonding

Table 4.5: Summary of FEA Results for Lateral Loading

Chapter 5: Manufacturing Process

The development of the manufacturing method consists of choosing which process will be used to assemble the composite materials and the inserts together and how to shape the part to its final shape. The choice of process depends on past experience, production rate, shape of the part and quality control.

5.1 Manufacturing Process Choice

The process chosen is a closed mould VARTM (vacuum assisted resin transfer moulding) for a one-piece carbon fork with a foam core. The steps for developing this particular manufacturing process are:

- Choice of the injection system
- Choice of materials (carbon fibre, epoxy)
- Design of the core
- Design of the carbon preform
- Design of the mould
- Final machining
- Finishing

5.2 Injection System

The choice of injection system is based on part and production parameters.

- Type of matrix to inject
- Volume of resin
- Temperature of injection
- Injection pressure

- Type of injection control required (volumetric or injection pressure)
- Maintenance of the machine
- Production rate
- Number of different parts to produce
- Time of injection
- Vacuum assist

The injection system required for this project is one designed for research and development of small composite prototypes. The versatility of the system has to be such that the type of resin, the volume, pressure and temperature of injection can be monitored and modified easily. Generally, the matrix will consist of two-part epoxy resins used in a range of temperatures between room temperature and 350°F (175°C). The volume of resin required to manufacture one fork is around 200cc. The pressure of injection has to be changeable in order to optimize the process.

One injection system compatible with the project parameters is the **Radius 2100cc RTM Injection Cylinder** made by **Radius Engineering** [18]. The injector satisfies the requirements for this project:

- 2100cc volume capacity
- Pneumatic piston
- Controlled temperature heated cylinder up to 350°F
- Volume display for resin in cylinder
- Manual pressure control
- Ease of cleaning
- Positive seal for vacuum and pressure
- Low cost
- Availability

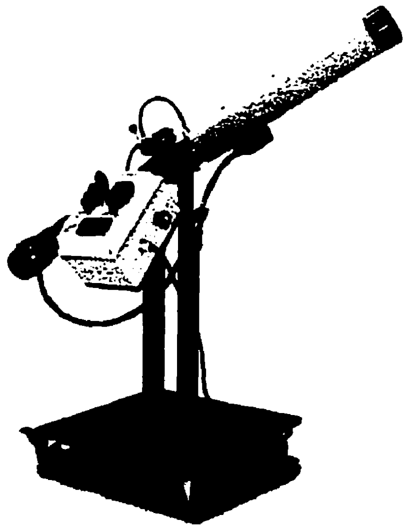

Figure 5.1: Radius Engineering 2100cc RTM System

5.3 Material Selection

The fork is constructed solely with carbon fibres and epoxy resin. In order to achieve the desired design, many characteristics are sought during the material selection phase. The first and most important one is the formability of the carbon fibre arrangement. The different configurations of fibres available on the market lead to infinite possibilities, but only a few permit keeping the integrity of the fibres and in the end the strength of the part. Some shapes are not very suitable for composite design. Sharp edges or small corner radii are problematic since the fibres tend to break or bend and cannot transmit the load anymore.

In this case, the major concern is the change in effective diameter along the fork legs. The cross-sections taper down from an elliptical section at the fork crown to a round section at the dropouts. It is very difficult to have continuous fibres when a part is tapered. With woven fabric, a triangular pattern is needed to conform to the shape, but then, there are some interrupted fibres along the leg of the fork as well as creation of a seam. Another problem resides in the layup of the fibres since it is complicated to place many layers while alternating proper overlap and respecting the design integrity.

Nevertheless, layups using woven fibreglass material were tried. The results, as mentioned before, were that it was tricky to cut the dry fibre patterns and to assemble them. Also, it was very difficult to kept the fibres oriented when the preform was placed in the mould.

On the other hand, braided materials are better suited for tubular applications and can be used easily for tapered shapes. The fibres are continuous since the braided carbon tubes conform to the change in relative diameter. The fibre angle as well as the mechanical properties of the braid also change proportionally with a change in the base diameter (See figure 5.2 and Table 5.1). Typically, braided material comes unstretched (base diameter) at a 45° fibre angle with the following properties:

- Longitudinal modulus: 3.47 msi (23.9 GPa)
- Transverse modulus: 3.47 msi (23.9 GPa)
- Shear modulus: 5.17 msi (35.6 GPa)
- Longitudinal tensile strength: 35 ksi (241.3 MPa)
- Transverse tensile strength: 35 ksi (241 MPa)

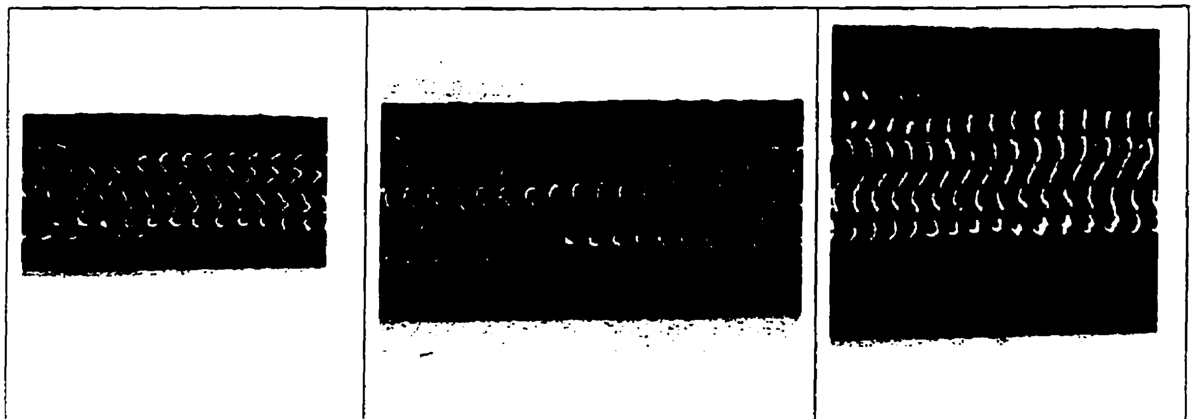

70% reduction in diameter 30° fibre angle	Braid at base diameter 1.25" (31.8mm) 45° fibre angle	130% stretch in diameter 65° fibre angle

Figure 5.2: Braid Material at Different Levels of Stretch

% of base Diameter	Angle	Length/yield*	Areal weight/ply thickness*	Axial modulus**	Transverse modulus**	In-plane shear modulus**	Axial tensile strength**	Transverse tensile strength**
130	66.8°	-44	38	-53	242	-38	-73	297
120	58.1°	-25	11	-41	110	-16	-60	138
110	51.1°	-11	2	-24	39	-3	-37	55
100	**45°**	**0**	**0**	**0**	**0**	**0**	**0**	**0**
90	39.5°	9	2	34	-22	-3	49	-34
80	34.4°	17	7	81	-36	-10	105	-54
70	29.7°	23	16	139	-45	-21	170	-65
60	25.1°	28	30	210	-51	-33	254	-71
50	20.7°	32	51	286	-55	-45	365	-75
40	16.4°	36	84	356	-58	-56	508	-78
30	12.2°	38	141	412	-60	-66	627	-80

* Values expressed are % Greater / Less than at ±45°

** Values expressed are % Greater / Less than typical laminate properties at ±45°

Table 5.1 Braid Parameters as a Function of Change in Relative Diameter

The values found in table 5.1 are from the carbon supplier for this project [41]. More information can be found in Appendix A. In the fork, the major constraints are mostly axial; therefore, the braid dimension should be such that the base diameter is reduced along the tapered sections of the fork in order to optimize the properties of the material. The fork blades start with a .591 inch (1.5 cm) diameter at the dropouts and blend into an elliptical cross-section with major axes a = 1.390 inches (3.53 cm) and b = 0.787inches (2 cm) for the sides (See figure 5.3).

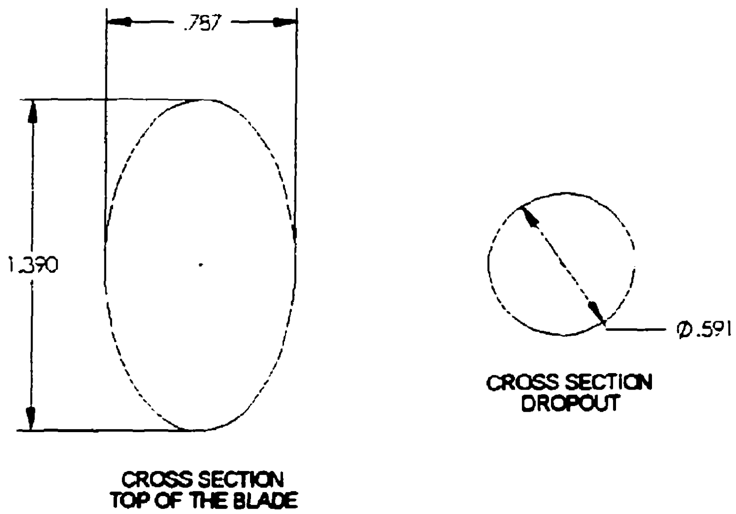

Figure 5.3: Fork Blade Cross Sections

The perimeter of the elliptical section is 3.486 inches (8.85 cm), which can be translated to a relative diameter of 1.110 inches (2.82 cm). The braid sock starts with a diameter of 1.110 inches (2.82 cm) and tapers down to a diameter of .591 inch (1.5 cm). The carbon formats chosen for the construction of the fork are layers of biaxial braid with fibres at ±45° and unidirectional braid. The UNIMAX™ material is a tube of unidirectional fibres along the axis of the tube [42]. The fibres are maintained together with a small elastic in the radial direction. The elastic allows the tube to stretch to larger diameters. Biaxial braid is also available in standard size under the trade name: GAMMASOX [43].

The tapered shape dictates which dimension of braid can be used in the carbon layup. UNIMAX™ comes in a dimension which is best suited for a diameter of .75 inch (19.1 mm) but can also conform to diameters from .38 inch (9.7 mm) up to 1.5 inches (38.1 mm) (see Table A.1 in Appendix A.) The diameters for that dimension fall in the range needed for the fork shape. The braided carbon biaxial sleeving comes in three different weights: light, medium, heavy, and the base diameter dimensions come in increments of 0.25 inch (6.4 mm). In order to satisfy the diameter range without stretching the base diameter, the material selected is a GAMMASOX™ heavy weight with a base diameter of 1.25 inches (31.8 mm) (See Table A.2 in Appendix A). The two blade layups meet at the crown and penetrate into the steerer tube to form the carbon reinforcement. One more layer of biaxial braid is used to cover the crown region.

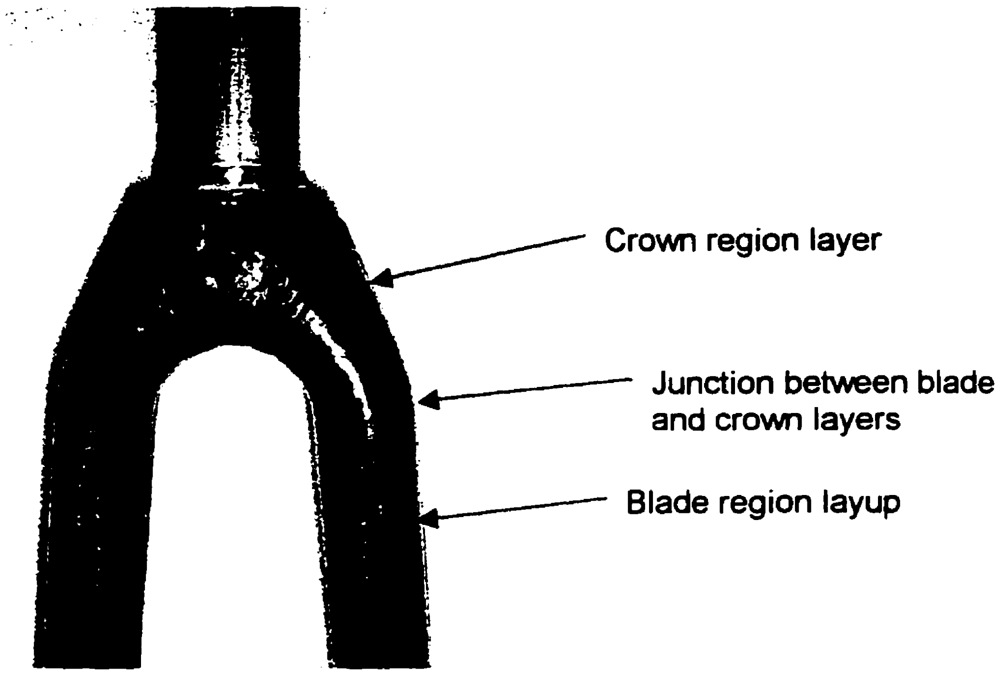

Figure 5.4: Fork Crown Close Up

Supplier	Product Code	Description	Base Diameter	Angle
A & P	UNIC7519	Carbon UNIMAX	0.75" (19.1mm)	0
A & P	P56L125X	Carbon biaxial sleeving	1.25" (31.8mm)	45
A & P	U57L200X	Carbon biaxial sleeving	2" (50.8mm)	45

Table 5.2 Carbon Fibres Braid Description

Now that the carbon fibre is selected, a suitable epoxy is needed to complete the composite structure. In order to be compatible with the RTM process; an epoxy resin has to meet various parameters.

- Mechanical properties
- Viscosity
- Gel time
- Temperature of injection
- Temperature of post cure
- Curing time
- Thermal expansion
- Colour

	Ciba Chemicals		**Dow Chemical**	**Resolution**
Epoxy resin	TDT177-114	Resinfusion™ 8601	D.E.R.™ 383	EPON® resin 862
Hardener	HY 956	Resinfusion™ 8602	D.E.H.™ 24	EPI-CURE® W
Specified use	Laminating	Infusion - RTM	Laminating	RTM
Colour	Transparent	Transparent	Transparent	Light orange
Viscosity at RT	800 cP	175 cP	1650 cP	2200 cP
Gel time at RT	38 min	70 min	40 min	N/A
Viscosity at 120 C	N/A	N/A	N/A	10 cP
Gel time at 120 C	N/A	N/A	N/A	N/A
Cure schedule	24 h	24h at RT	16 h at RT	8h at 250F (120 C)
Post cure	7 days at RT	3 days at RT	3 h at 220 F (100 C)	None
Flexural Strength	N/A	11 013 psi (76 MPa)	17000 psi 117 MPa)	18 000 psi 124 MPa)
Tensile Strength	N/A	7 871 psi (54 MPa)	10 900 psi (75 MPa)	12 000 psi (83 MPa)
Comp. Strength	N/A	15 410 psi 06 MPa)	15 800 psi (109 MPa)	N/A

Table 5.3 Epoxy Systems Specifications [44-53]

All three systems are suitable for VARTM process. The Resinfusion™ was tried but it was abandoned because of its slow cure time and lower mechanical properties. The D.E.R.™ and D.E.H.™ samples were not received in time for trial so the EPON® and the Ciba TDT177-114 systems were used to construct the prototypes. However for manufacturing, the Dow system might be preferred since it is more affordable.

The remaining sections in the development of the manufacturing process are essential since they determine the shape of the fork.

5.4 Bladder System Development

In order to mould a composite part, the carbon preform has to conform to the shape of the mould cavity. In VARTM, two common options are used to help make a "hollow" part: internal bladder or foam core. An internal bladder system is very interesting since a pneumatic pressure can be applied on the laminate after the injection thus increasing the compaction of the fibres.

The method used to create the internal bladder was to mould liquid rubber onto a cast of a fork shape that was smaller than the actual fork shape. First the internal surface of the mould is covered with a calibrated wax (Sheet of wax with a precise thickness) [54] to simulate the thickness of the layup and then the mould is closed and sealed. The next step is to pour liquid polyurethane [55] in the mould to cast the fork shape minus the thickness of the layup. This gives a solid mandrel onto which a bladder can be formed.

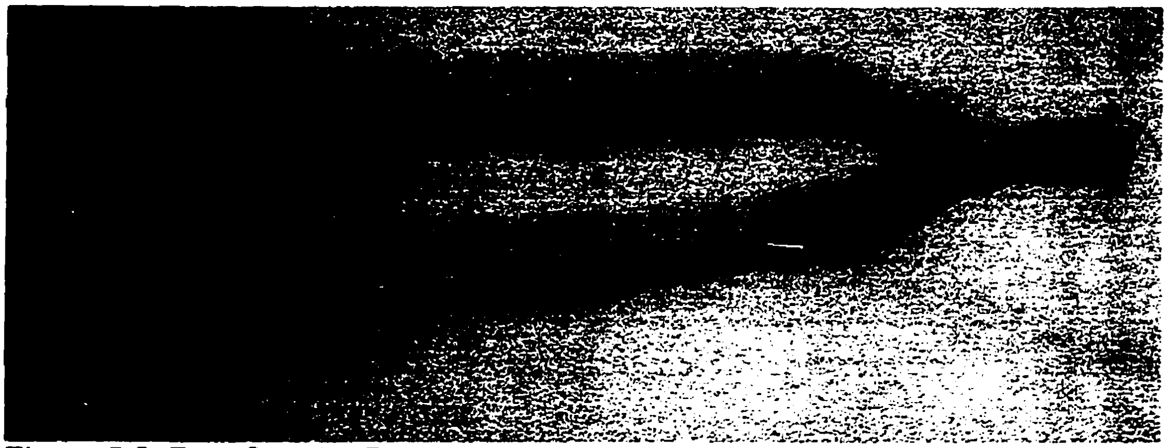

Figure 5.5: Fork Cast for Bladder Moulding

Two products were tried to make the bladder. The first one, Cleartex™ [56], is a synthetic rubber which can withstand a large elongation before rupture. Practically, the Cleartex™ could not be applied correctly to the fork cast because of its low viscosity. Another product was tried, liquid silicone [57], but then after making a bladder, the shape of the cast had some critical areas (tight corners) where the bladder would rupture. The proper technique to make the bladder would have been rotomoulding [58], which consists of placing a mould in a special machine that turns in all directions while the liquid rubber solidifies with equal thickness on the whole internal surface. The equipment necessary for this technique was not accessible; therefore, the final the solution adopted was to use surgical tubes.

The bladder system was tried in wet layup with woven glass fibres. Fibreglass was used because it cost less than carbon. Two attempts were made but each time the bladder burst. The rupture can be explained in three possible ways. First, the bladder was chemically attacked by the liquid epoxy. Second, the bladder stretch was more then it could support (the tube used had a 400% elongation rating before rupture). Third, the steerer tube insert damaged the bladder in the crown area. The most possible explanation is probably a combination of all three. The bladder stretched to its maximum in the crown area but not enough to break it. In fact, the preform with the bladder was placed in the mould and inflated without rupture. At the same time, the titanium insert induced a stress point were the bladder was elongated. Therefore when the epoxy was injected in the mould, it chemically attacked the bladder, which broke at its weakest point in the crown region (the tube was stretched, thus reducing the wall thickness.)

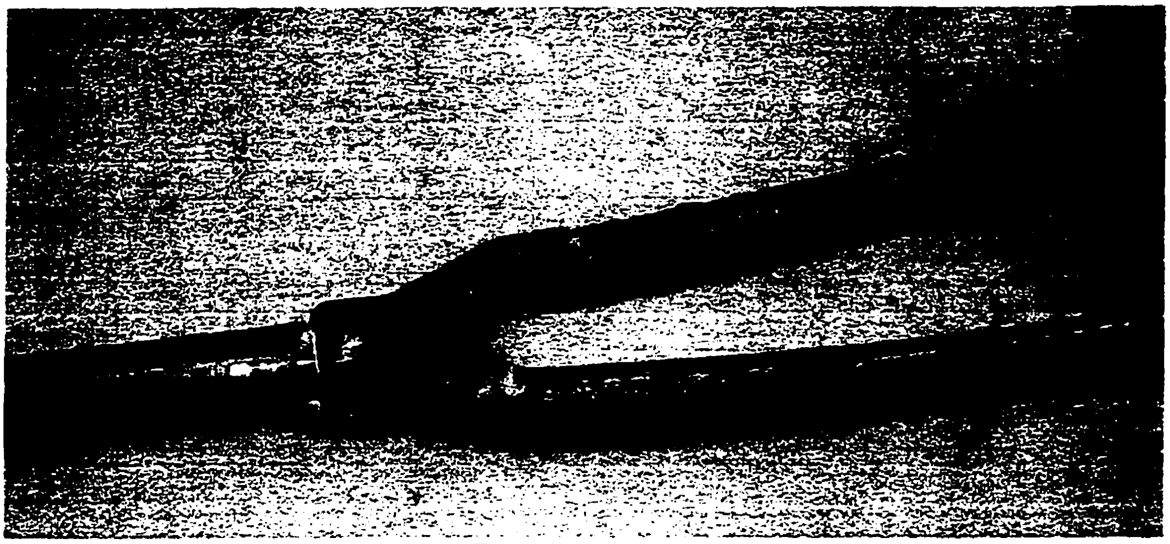
Figure 5.6: Prototype Made with Bladder.

After months of research into finding another material that would suit the characteristics for this bladder, none were found with enough stretch for the tapered legs or with appropriate chemical resistance for epoxies; therefore, the design was then oriented towards a foam core construction. This method is already in use by General Composites [59] and is proven to work with bicycle fork manufacturing.

5.5 Foam Core Development

The foam core is made of high-density polyurethane foam. This type of foam is suited for composite applications since it is a closed cell structure and does not soak up resin, thus, does not increase the weight of the part considerably [60]. The foam core is machined to the shape of the fork less the thickness of the carbon layup.

The core of a composite part is essential to its shape and its structural properties. In the fork, the foam acts as support for the carbon preform, but more crucially, the shape of the foam core controls the gap to be filled with fibres and epoxy in the mould thus controlling the fibre volume in the fork. As mentioned in chapter 2, the final fibre volume has a direct effect on the performance of the composite part. Therefore, special attention is required when designing the foam core. However, the complexity of the fork shape especially in the crown region makes it almost impossible to produce a foam profile with a perfect core shape. Therefore, there will be regions in the crown that will be "resin rich" (where the fibre volume is considerably lower than designed.) Before giving shape to the core, the fork layup has to be defined since the surface of the mould is fixed, and any changes in the layup affect the shape of the foam core.

The layup chosen in Chapter 4 will be used to make the prototypes. However, some modifications are made to the layup in order to adapt to braid material. As the relative diameter of the fork tapers down at the dropouts, the ply thickness increases and the properties of the braid increase significantly (See Table 5.1). Therefore fewer layers of carbon fibres are needed in the dropout regions. The layup is then divided to the following sections: the crown has 8 layers, the blade has 4 layers and now the dropout region has 2 layers.

All three regions will have different thicknesses, and even within one region the ply thickness will vary according to the relative diameter of the fork cross-section. Since the fork tapers down from the top of the blade to the dropout, the layup will gradually increase in thickness along the blade. Each cross section of the foam core has to be calculated from the values in Table 5.1 and Table A.1.

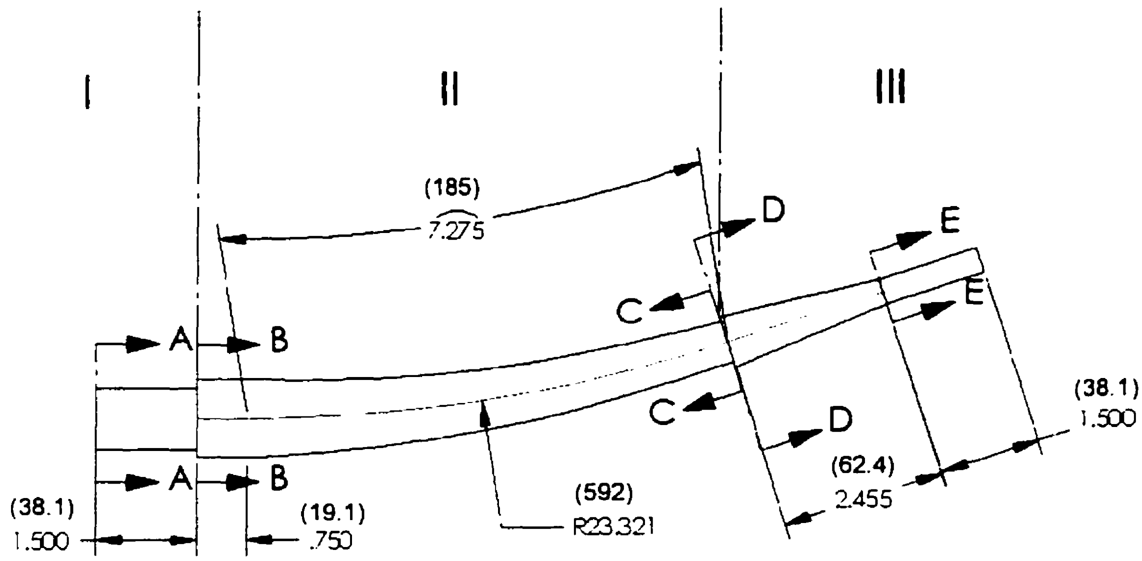

Figure 5.7: Foam Core Specifications

Region	Relative diameter Inch (cm)	Layer	Type	% of Relative Diameter	Thickness Inch (cm)
I	1.117 (2.84)	I	Biaxial	90	0.034 (0.09)
	1.050 (2.67)	II	Uni		0.022 (0.06)
	1.005 (2.55)	III	Uni		0.023 (0.06)
	0.959 (2.43)	IV	Biaxial	77	0.036 (0.09)
		Ply Thickness at section B-B :			**0.115 (0.29)**
	0.888 (2.26)	V	Biaxial	71	0.037 (0.09)
	0.813 (2.07)	VI	Uni		0.027 (0.07)
	0.760 (1.93)	VII	Uni		0.028 (0.07)
	0.704 (1.79)	VIII	Uni		0.032 (0.08)
		Ply Thickness at section A-A :			**0.238 (0.60)**
II	0.802 (2.04)	I	Biaxial	65	0.039 (0.10)
	0.723 (1.84)	II	Uni		0.030 (0.08)
		Ply Thickness at section D-D :			**0.069 (0.18)**
	0.663 (1.69)	III	Uni		0.035 (0.09)
	0.594 (1.51)	IV	Biaxial	45	0.053 (0.13)
		Ply Thickness at section C-C :			**0.157 (0.40)**
III	0.591 (1.50)	I	Biaxial	45	0.053 (0.13)
	0.485 (1.23)	II	Uni		0.048 (0.12)
		Ply Thickness at section E-E :			**0.101 (0.26)**

Table 5.4: Details of Ply Thickness

5.6 Mould Design

Primarily, the mould fixes the final outer shape of the part but many features are necessary for proper function of the manufacturing process. The production of composite parts by VARTM requires a mould to place the fibre arrangement and inserts and to inject and cure the epoxy. The mould shape consists of a female cavity of the fork with injection and vacuum ports and a clamping mechanism.

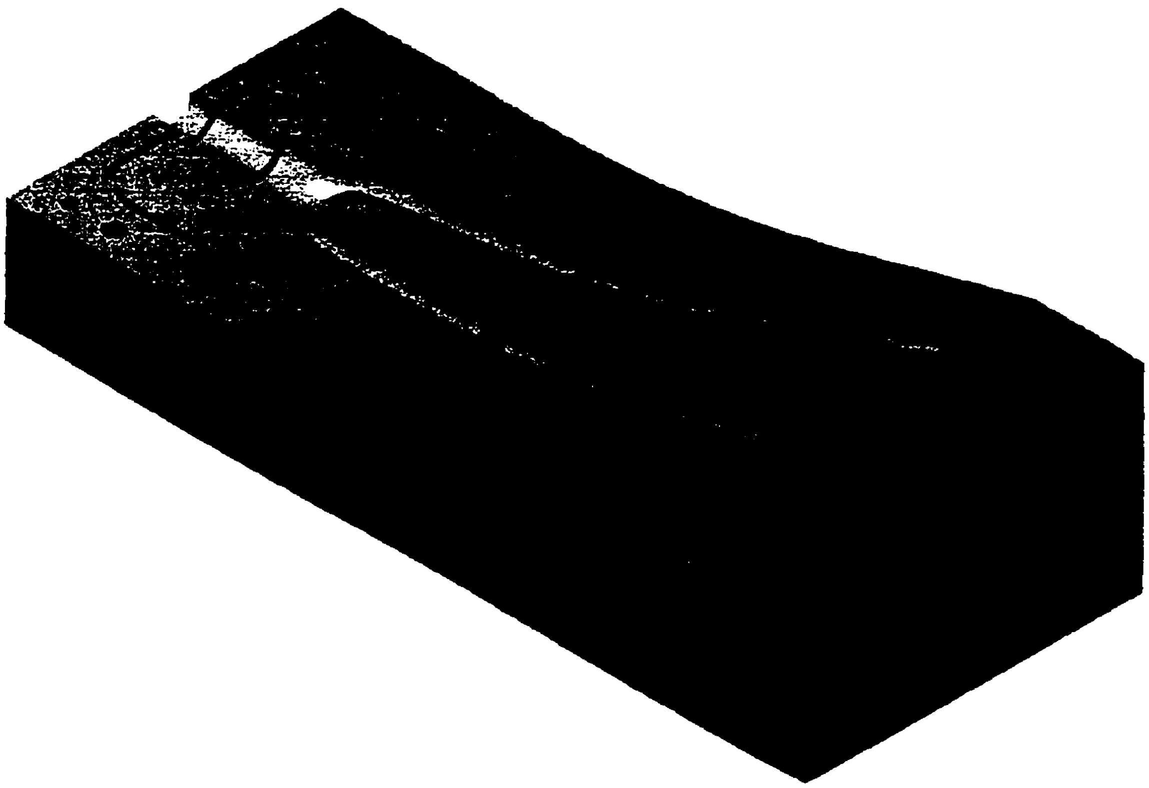

Figure 5.8 Bottom Half of the Mould (CAD)

Female Cavity

The mould cavity is designed to shape the outer surface of the fork and one important aspect is to be able to place the preform in the mould. The fork has two regions with sharp corners: the crown bearing race and the dropouts. Unfortunately sharp corners are impractical to mould because the fibres cannot be easily placed in corners. Furthermore, the braid material used in the making of the fork cannot be cut to the exact shape because the fibres are not stable near the end of the cut. Therefore, extra material is moulded and removed in the post machining sequence to form the sharp corners. In order to place the extra material in the mould, pockets are added in the mould at those regions.

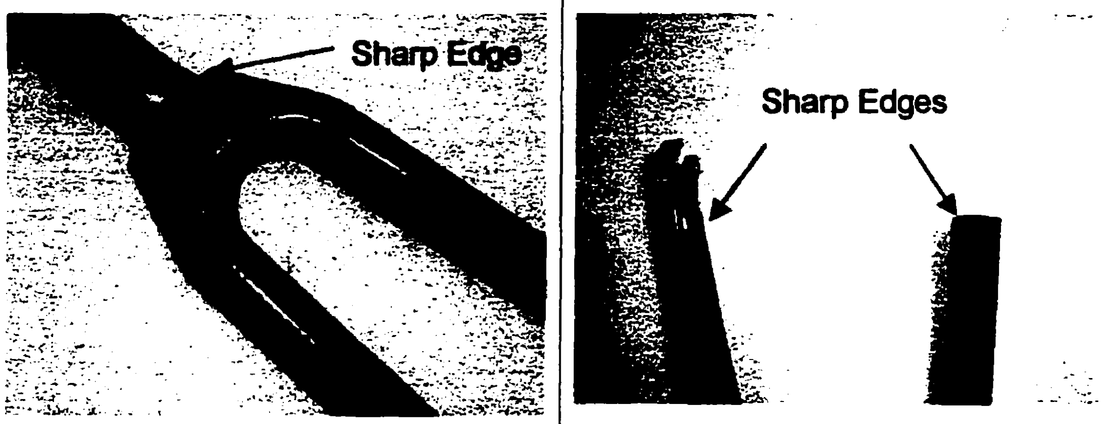

Crown edge	Dropout edges

Figure 5.8: Sharp Corners of the Fork.

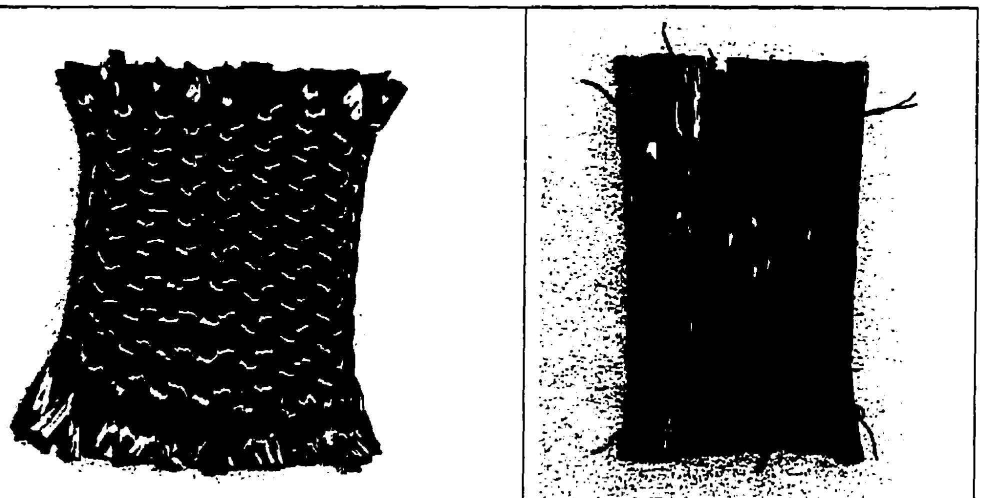

Biaxial braid material	Unidirectional braid material

Figure 5.9: Braid Material Manipulation and Extra Material at the End of Cut.

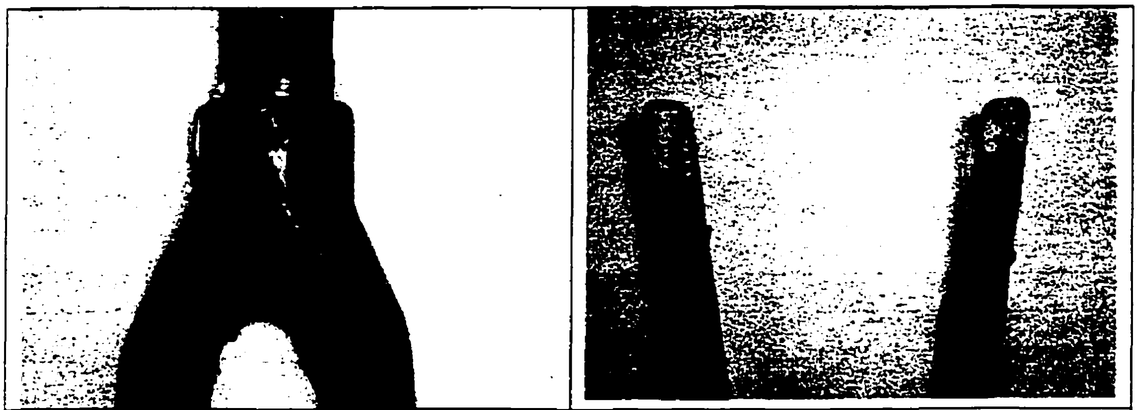

Fork Crown extra material	Fork dropout extra material

Figure 5.10: Fork with Extra Material before Final Machining

Seal

In the first stage of the injection process, the mould is placed under vacuum to remove all the air that could be trapped in the resin and help the resin flow by creating a near zero atmosphere backpressure on the flow front. When vacuum pressure is reached, the resin is injected until the mould is completely full and then a hydrostatic pressure is applied in the mould with the injection cylinder to increase the part quality and prevent any voids. These two consecutive steps require that the mould keep its seal integrity throughout vacuum and pressure. An O-ring channel is designed and machined around the cavity to assure the seal.

Closing Mechanism

The mould is subjected to high forces while under hydrostatic pressure and sufficient closing power is required to prevent deformation and opening of the mould. Two toggle clamps are used for easy closing and eight bolts are placed on the mould for a complete mould seal. The toggle clamps are also used as handles to open the mould. The mould is placed on a hinge to facilitate the opening of the 40 Kg block of Aluminium. When closing the mould, two locating pins assure the alignment of the two halves.

Injection and Vacuum Ports

The injection system is connected to the mould with a disposable nylon tube (Teflon is used for high temperature). The tube goes all the way to the cavity. It is held in place by a compression fitting which also assures a good seal for both vacuum and pressure with its pipe thread. The vacuum pump is connected in the same fashion.

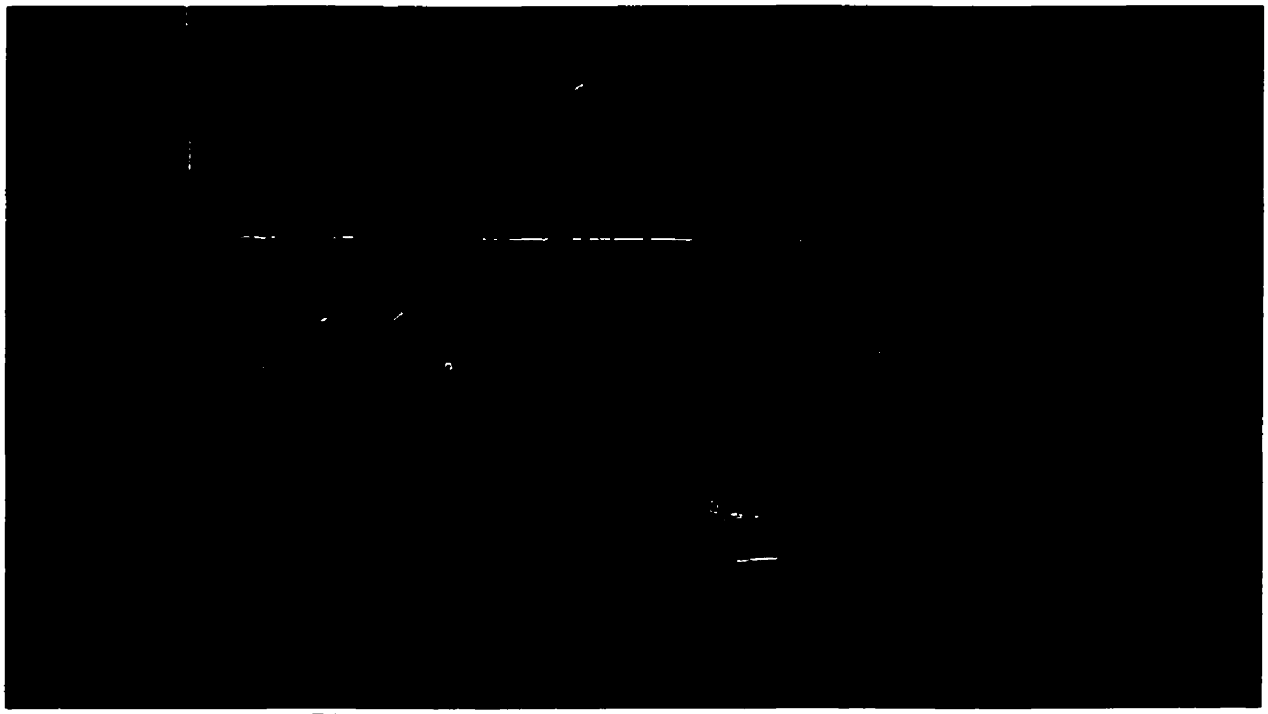

Figure 5.11: Process Diagram

Insert Alignment

Metallic inserts can also be placed inside the mould. For the fork, the steerer tube assembly is placed in the mould since it is part of the layup with the steerer tube reinforcement. The dropouts, however, are bonded to legs after the fork is fully cured. The steerer tube is located in the mould with a locating pin that goes in the brake hole. This pin assures rotational as well as translational positioning.

A summary of mould features for VARTM is illustrated in figure 5.12.

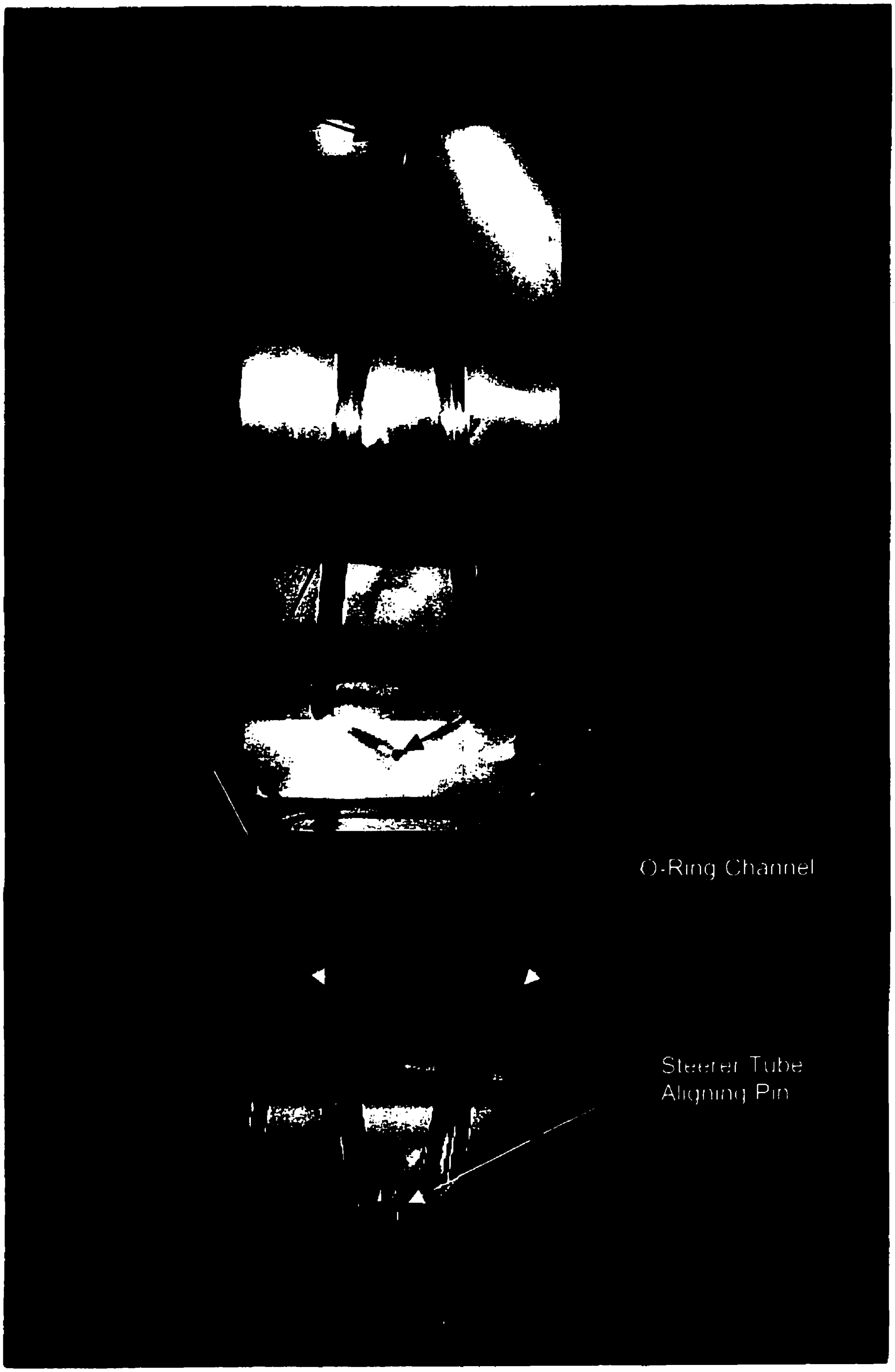

Figure 5.12 Mould Details

5.7 Final Machining

Final machining of the fork consists of removing the extra material left from the injection, drilling the brake hole and bonding of the dropouts. The pocket at the shoulder of the fork is removed on a lathe with a regular parting tool and the steerer tube insert is machined to tolerances for press fitting the bearing race. Then the brake hole is drilled on a regular milling machine to fit a 6mm bolt.

The ends of the fork legs are longer than necessary. They need to be cut in a jig using a composite diamond disk cut off blade. The use of this type of blade prevents edge delaminations from occurring at the cut end. Then a hole is bored at the end for inserting the dropouts. The hole is larger than the dropout post to allow a bond thickness of between .005 and .015inch (0.12 and 0.38mm) and to allow precise alignment of the dropouts. The dropouts are then bonded to the legs using a precise bonding fixture.

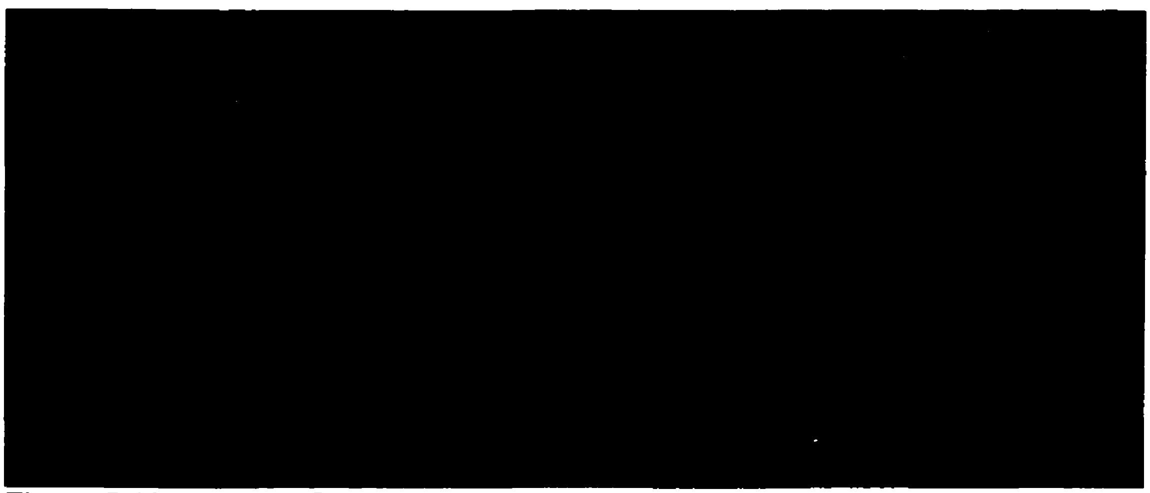

Figure 5.13 Dropouts Bonding Fixture

5.8 Finishing

After the final machining, some finishing is still needed for the final look of the fork. During the injection, a thin film of epoxy called mould flash is formed between the two halves of the mould. This film breaks easily, but it has to be shaved off at the fork surface. Usually a razor blade or a light sand paper is sufficient to take off the flash.

The surface of the fork can only be as good as the surface of the mould. The mould is made of aluminium so it is easy to obtain a mirror finish but practically this finish does not last very long without frequent touch ups. Also a release agent is applied on the mould surface to assure demoulding of the fork [61]. This agent makes the mould surface blush so a clear finish on the fork is difficult to obtain directly out of the mould. A crystal finish is a great added value to a composite part so the fork can be lightly sanded and then sprayed with a clear coat.

Chapter 6: Experiments and Testing

After developing the manufacturing process, prototypes were fabricated to verify the validity of the design and manufacturability of the fork. The prototypes were tested statically and in fatigue to determine the structural properties and examine the mode of failure.

6.1 Fabrication of Prototypes

The first injections were performed to get familiar with the procedure and equipment. Therefore fibreglass and rough foam shapes were used since the performance was not a concern for the initial prototypes (see figure 6.1).

Figure 6.1: Prototypes Made with RTM Using Woven Fibreglass.

The fibreglass prototypes were very helpful for understanding the VARTM process. Fibreglass becomes transparent when wetted with epoxy, so it is possible to detect problematic areas of the fork in terms of locating air bubbles in the resin as well as insert and foam alignment (See figure 6.2).

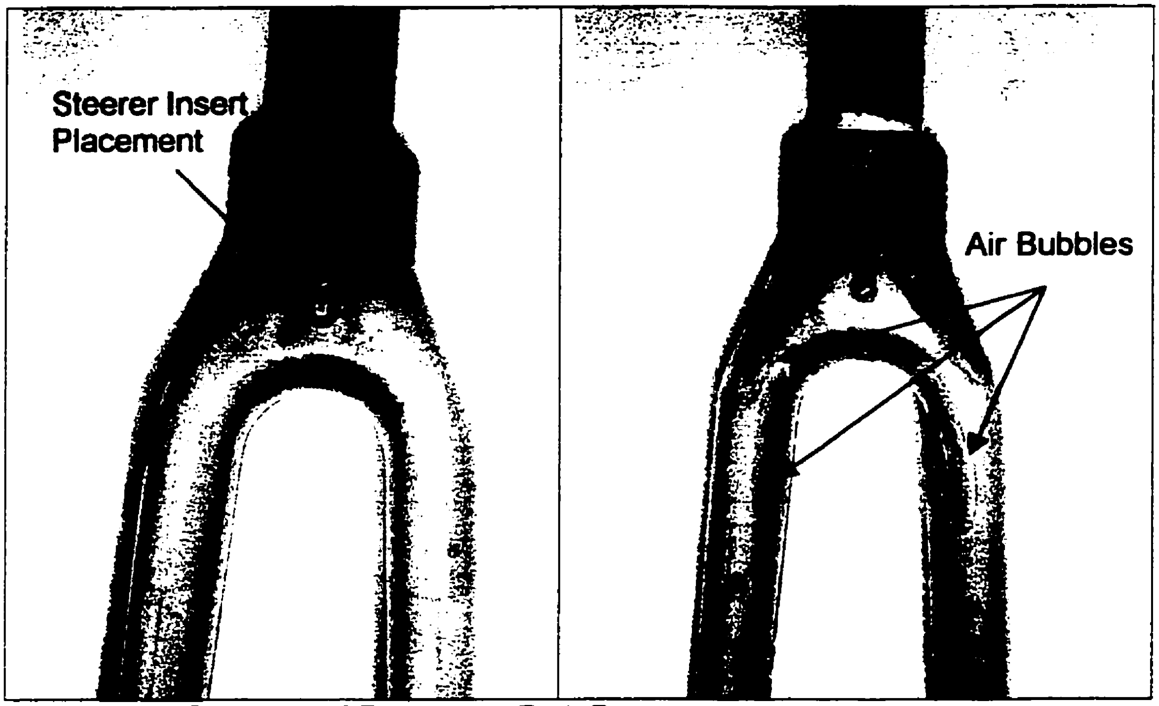

Figure 6.2: Close up of Fibreglass Fork Prototypes

The air bubbles can be removed by degassing the epoxy prior to the injection. Degassing consists of removing any gas (air and solvent) trapped in the resin by placing it under vacuum to pull the gas or under pressure to push the gas out. Applying a hydrostatic pressure at the end of the injection with the cylinder and maintaining the pressure until the gel time will also reduce the number of air bubbles [18].

Four carbon prototypes were built (See figure 6.3). Two had steel steerer inserts because titanium was not available during the fabrication of the first two prototypes. The first fork used the same layup as described in section 5.4, and the second used one less unidirectional layer in the steerer tube. This was tried because the carbon material was really tight in the steerer region and one less layer would facilitate the layup sequence. The last two forks were produced with Titanium inserts and the full layup of section 5.4. Different epoxies were tried to evaluate their ability to be injected and their mechanical properties.

Serial Number	Insert Material	Layup Sequence	Epoxy System
Fork-001	Steel	Biaxial + 3Uni	TDT177 114
Fork-002	Steel	Biaxial + 2 Uni	TDT177 114
Fork-003	Titanium	Biaxial + 3Uni	Epon
Fork-004	Titanium	Biaxial + 3Uni	Epon

Table 6.1: Fork Material Description

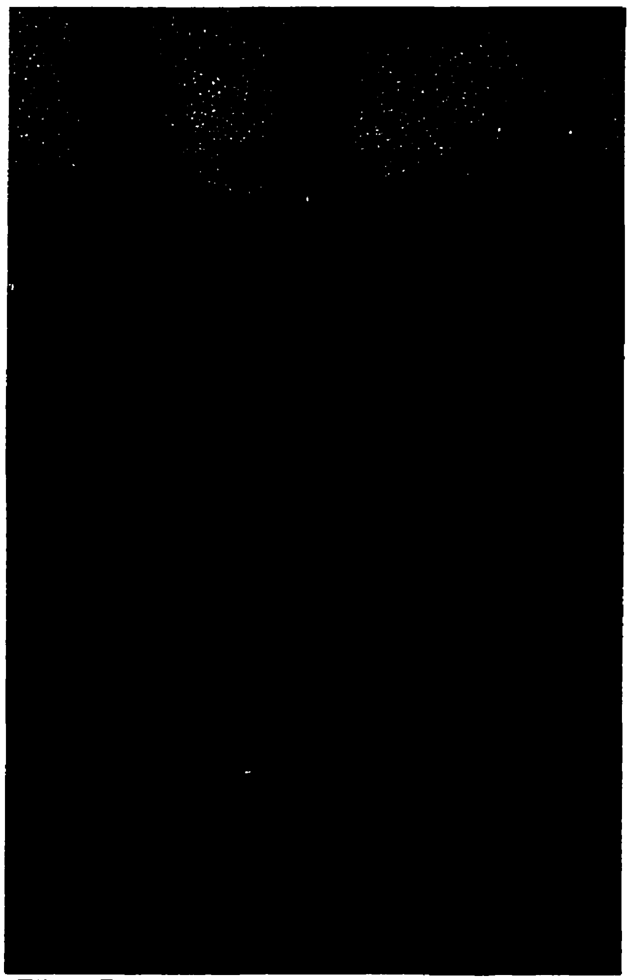

Figure 6.3: Carbon Fibre Prototypes.

All four prototypes were made successfully and were tested.

6.2 Experimental Apparatus

An important step in the design of a fork is to evaluate its performance. The performance of a component is measured first with regard to itself (does it meet the design criteria defined) and secondly, in comparison with other similar existing products.

Two types of tests are performed on the fork to determine its quality. They are the destructive and the non-destructive tests. The non-destructive test determines the frontal stiffness of the fork. The destructive test consists of repeated frontal impacts applied to the fork to determine a fatigue life.

McGill University students developed testing equipment to test bicycle forks [35-37]. Over the years, some modifications were made to the fixture to refine the procedures and simulate more realistic test conditions. The piston was changed and the piston holder was redesigned and rebuilt for the purpose of this study. The previous piston had a 2 inch (5cm) displacement range and could not perform complete fatigue tests to the point of complete fork failure (Details in section 6.4.) The new piston now has a 4 inch (10cm) displacement range. The old piston holder could not rotate freely on its base thus increasing the stiffness of the fork unrealistically due to friction. The new piston is now mounted on a large bearing to allow free rotation during the fork displacement. Finally, the test fixture was completely rebuilt to facilitate the adjustment of the piston and the tested components [35].

Figure 6.4: Picture of Test Fixture

6.3 Non-Destructive Test Descriptions

The frontal stiffness test evaluates the resistance to frontal or "brake" loadings. The test consists of pulling on the fork with the pneumatic piston at a 73degree angle from the steerer tube alignment direction and applying the same loading conditions as in the finite element analysis (See figure 4.4).

The load is applied at the centre of the test fixture axle in a ramp test. The time for the ramp is 30 seconds and the maximum load is 1000N. Deflection of the piston is measured. The stiffness is calculated from the ramp test slope on the load deflection curve.

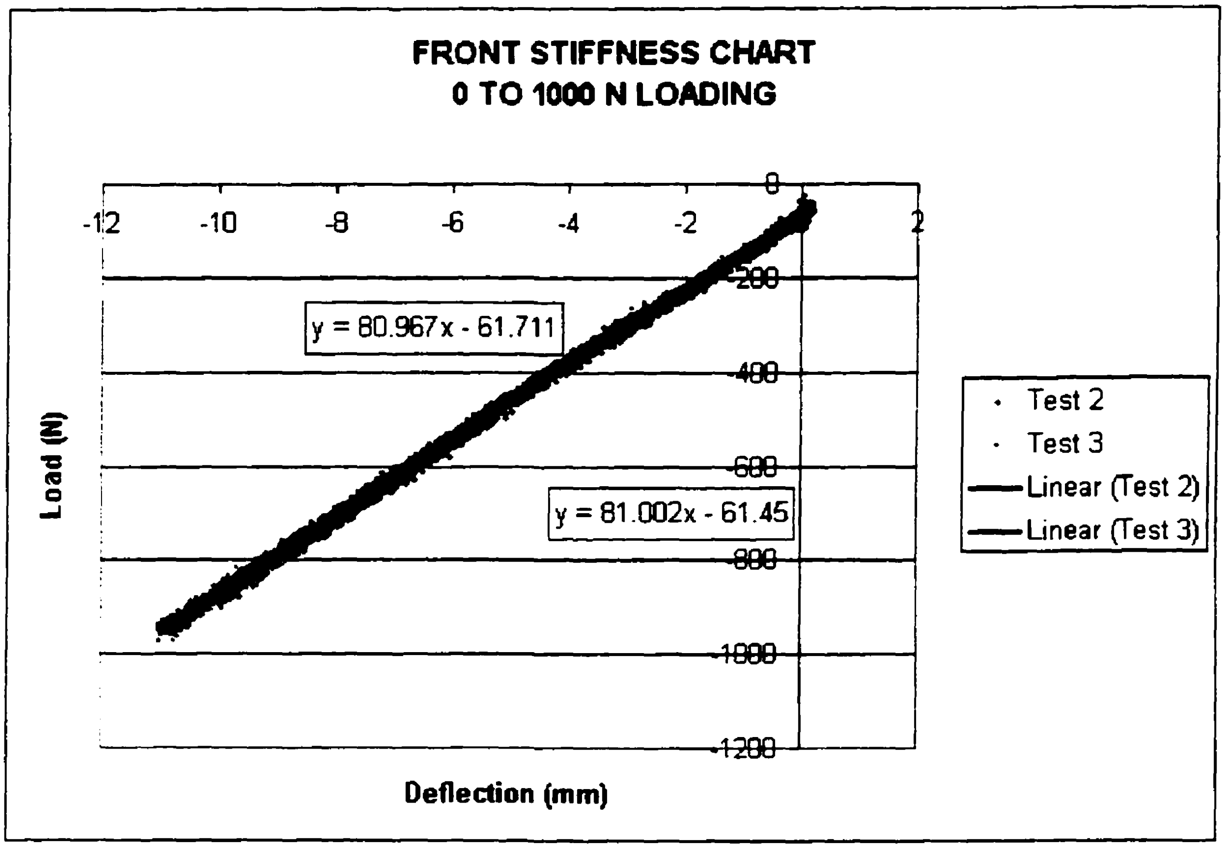

Figure 6.5: Front Stiffness Chart Example

6.4: Destructive Fatigue Test

The destructive test is a series of impacts applied consecutively. The frequency of the load application is approximately 0.66Hz. The peak load increases as the test evolves in order to achieve failure. The starting peak load is 1000 N, applied for 5000 cycles, and it is increased by 200 N every 5000 cycles. The test set-up is the same as in the front stiffness test. Near failure, the fork stiffness will decrease and the fork will eventually break. This type of loading simulates a frontal impact with the bicycle.

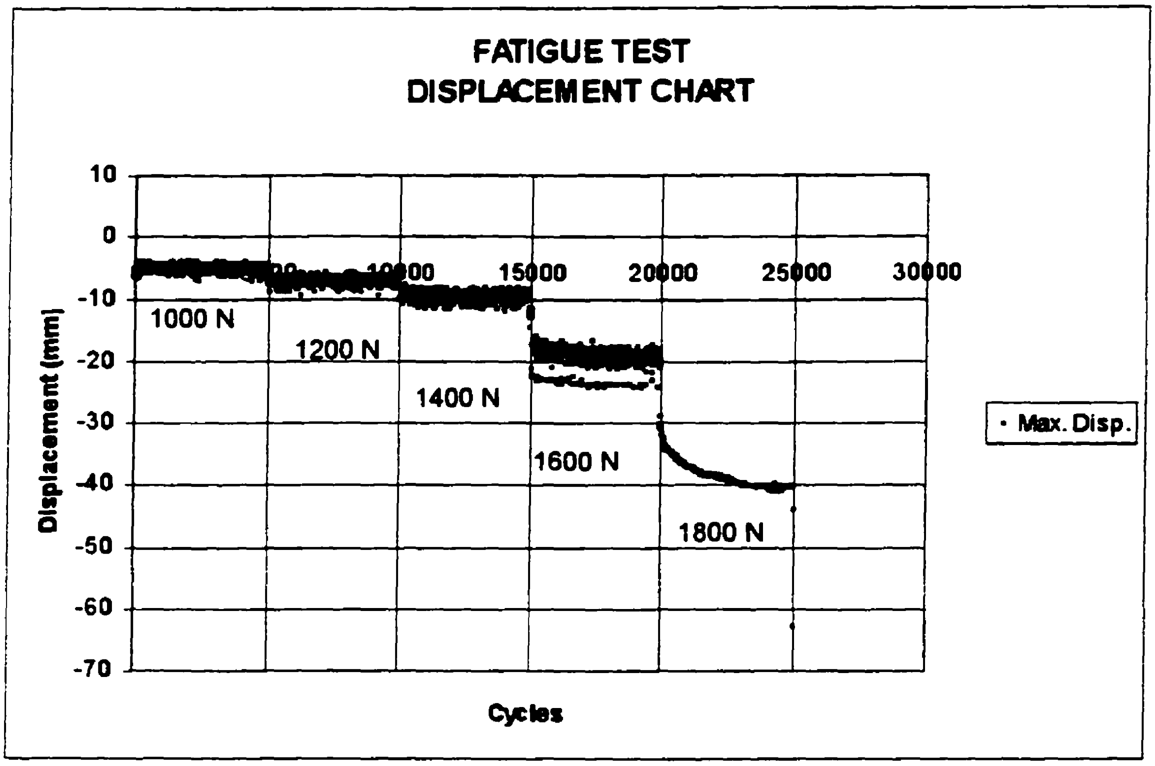

Figure 6.7 Fatigue Test Chart Example

The chart in figure 6.7 shows a typical test result of the destructive fatigue test. At low load levels, the maximum displacement stays relatively constant. However, during the critical load level (Shown here at 1800 N) the gradual deterioration of the fork leads to increasing maximum displacement while under constant load. Eventually, complete failure occurs when the fork can no longer withstand any more load.

6.5: Experimental Results

All four prototypes were tested as well as three Serotta F1 forks. This project is based on the redesign of the F1 fork in order to reduce its weight and increase its performance.

Serial Number	Description	Weight (g)	Steerer Material	Frontal Stiffness (N/mm)	Stiffness to Weigth Ratio (N/mm/g)	Fatigue test	
						Cycles	Final Load (N)
Fork-001	New Carbon	626	Steel	123	0.196	20 000	1600
Fork-002	New Carbon	632	Steel	93.5	0.148	5 700	1200
Fork-003	New Carbon	582	Titanium	98	0.168	8 600	1200
Fork-004	New Carbon	541	Titanium	102	0.189	16 900	1600
0101001	Serotta F1	685	Steel	115.9	0.169	50 000	2700
0101002	Serotta F1	690	Steel	111.7	0.162	45 000	2600
0101003	Serotta F1	723	Steel	128.4	0.178	50 000	2700

Table 6.2: Summary of Test Results

6.6 Experimental Results Discussion

The new carbon structure compares well with the old design in terms of rigidity. The first two prototypes have higher weight because they were made with the redesigned steerer tube insert in steel. The other two prototypes were made with metallic inserts made with titanium. The first fork has the highest frontal stiffness. The second fork has one fewer layer of unidirectional braid as reinforcement in the steerer tube, which explains a 24% reduction in frontal stiffness with the first one. Therefore, it is important to keep this layer in the steerer tube region. The third and fourth forks are identical in composition with their titanium insert and complete reinforcement layup as in the first prototype. They both have similar results for the front stiffness with an average stiffness of 100N/mm. This is a reduction of 19% compared to the fork with a steel insert. This difference was expected since titanium has a lower rigidity than steel. The fourth fork is lighter than the third one because the foam core geometry was adjusted for a better fibre volume. It did not affect the stiffness of the fork but reduced the weight by 7%.

The old carbon forks, the Serotta F1, have an average frontal stiffness of 118.7N/mm. The F1 fork is 16% stiffer than the new fork with titanium insert but the new fork with a steel insert is stiffer by 4%. The new fork also shows a weight reduction of 23% (comparison with the optimized fourth prototype). In term of performance, the new fork has an increase in stiffness-to-weight ratio by 11% when compared with the F1 fork.

The fatigue life of the new fork is considerably lower than of the F1 fork but compare similarly with other high performance forks available on the market (test data of other fork manufacturers cannot be published).

Moreover, the new fork with a titanium insert was road tested by a bicycle expert (Ben Serotta) and the rigidity of this new fork under real riding conditions was judged excellent. The "ride feel" of the new fork was characterized as "exceptional" and possibly better than the F1 fork due to its improved damping of road imperfections.

6.7 Carbon Structure Result Discussion

After the forks were tested, one fork, the Fork-002, was cut open to examine its composite structure and, if possible, the mode of failure. It was cut at the midplane. Figure 6.8 shows a cut out of the fork crown region. The different layers of carbon fibre can be seen by the reflection of light. The structure is almost voidless except in the resin rich region at the bottom arch of the crown (See figure 6.9).

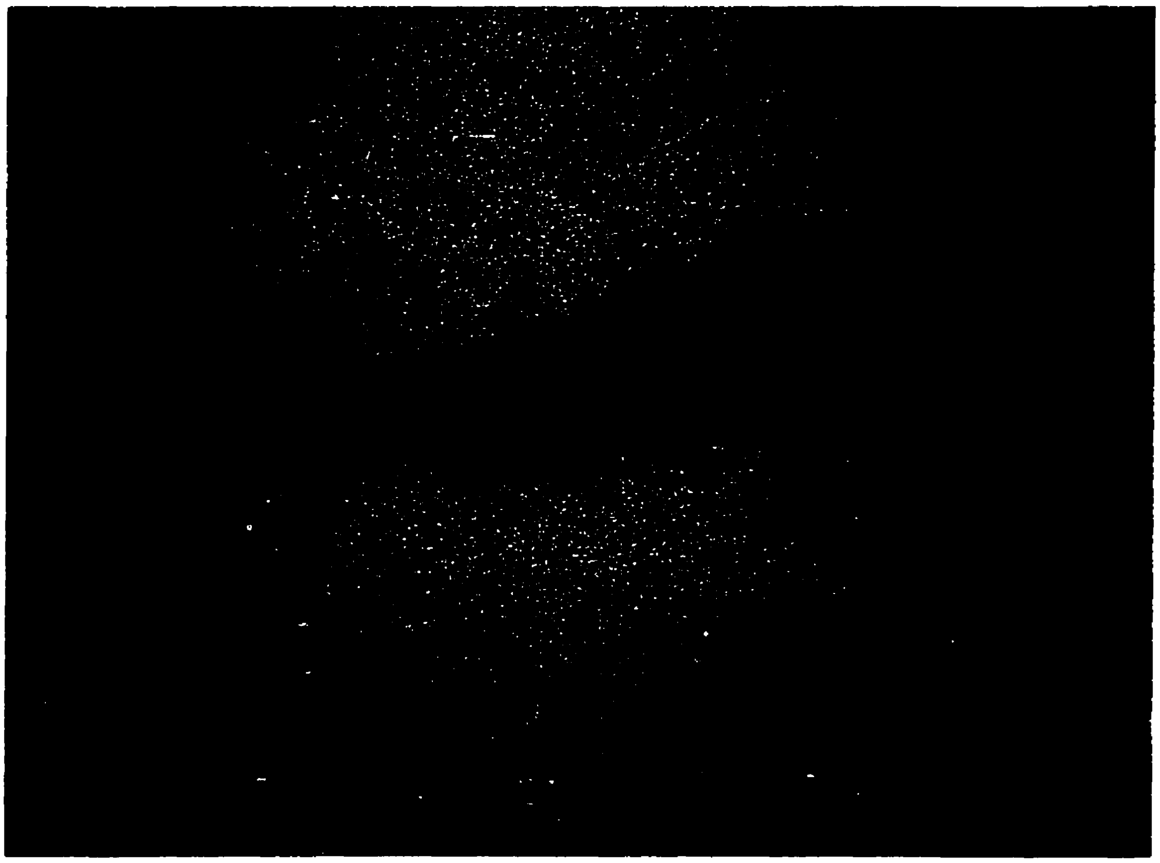

Figure 6.8: Fork Cut Out of Crown Region

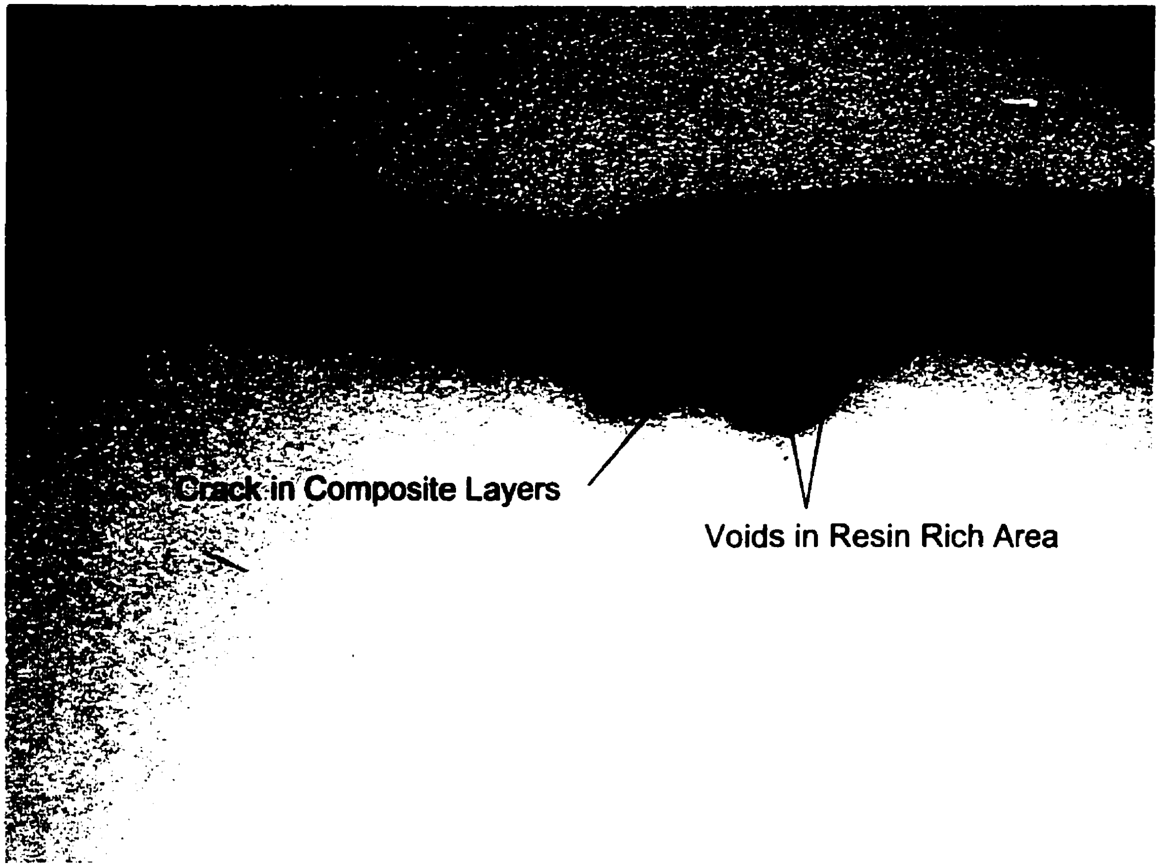

Figure 6.9: Close Up Of Fork Cut Out

Figure 6.9 shows considerable voids in the composites, which can diminish the performance of the fork. However, a failure crack is visually noticeable in the composite at the brake hole. This fracture occurred during the cycling of the fatigue test. The mode of failure observed experimentally correlates with the finite element analysis results. In chapter 4, it was noted that the maximum stress region for frontal loading was at the edge of the brake hole (See figure 4.14 and table 4.4).

Chapter 7: Conclusion

The present research has undertaken the redesign of a composite bicycle fork for both geometry and structure. A finite element analysis was performed on the new structure and showed the points of maximum stress. Simultaneously, a vacuum assisted resin transfer moulding (VARTM) manufacturing method was developed in order to transfer the technology for production. The method was used to make prototypes for experimental testing. Four structural carbon fibre prototypes were built and tested to verify both the manufacturing process and the performance of the composite construction. The VARTM process was proven to produce prototypes efficiently which can be transferred to production. The manufacturing process can produce forks at a competitive price.

The new fork design met the technical parameters set for this research. The fork has a 23% weight reduction with the old design. The overall efficiency of the fork, measured by stiffness-to-weight ratio, is also improved by 11%. The rigidity of the fork is 16% lower but is excellent under riding conditions. The fatigue life of the fork is reasonable for high performance composite fork. The mode of failure of the fork in fatigue corresponds with the stress regions found in the finite element analysis and is not catastrophic.

7.1 Contribution to Knowledge

This research presents the following original contributions:

- A high performance bicycle fork was created.
- A Titanium steerer tube reinforced with carbon fibre was able to replace a steel insert without compromising the structural integrity of the fork.
- The mode of failure of the fork was predicted with a finite element analysis and confirmed with experimental tests.
- A manufacturing process for VARTM was developed for prototype fabrication and commercial production.

7.2 Recommendations for Future Work

- Tension, compression and shear tests should be performed on test samples made with the VARTM process to obtain the mechanical properties of different combinations of braid material and epoxy systems necessary for the finite element analysis.
- An internal bladder system should be developed and incorporated in the manufacturing process in order to increase the fibre volume and therefore reduce the weight of the fork.
- Injection parameters can be optimized for better structural results and faster injection times.

REFERENCES

1. Serotta Competition Bicycle, Great American Bicycle Company, South Glen Falls.

2. Interbike 2000, Las Vegas, Nevada, September 2000.

3. "Bicycle," Microsoft® Encarta® Encyclopedia 2000. © 1993-1999 Microsoft Corporation.

4. Perry, David B., Bike Cult, Four Walls Eight Windows, New York and London, 1995, pp. 50-52.

5. Perry, David B., Bike Cult, Four Walls eight Windows, New York and London, 1995, p. 59.

6. "Aheadset", Cane Creek, 11 January 2001, <http://www.canecreek.com/index_as.html>

7. "About Composites", National Composite Center, 23 Feb. 2001, <http://www.compositecenter.org/>

8. "Plastics," Microsoft® Encarta® Encyclopedia 2000. © 1993-1999 Microsoft Corporation.

9. Strong, A.B., Fundamentals of composite Manufacturing: Materials, Method and Applications, Society of Manufacturing Engineers, Deerborn, Michigan, 1989, p. 17.

10. "Fibers," Microsoft® Encarta® Encyclopedia 2000. © 1993-1999 Microsoft Corporation.

11. Kaw, Autar K., Mechanics of Composite Materials, CRC Press, Boca Raton, Florida, 1997, p. 154.

12. Agarwal, Bhagwan D., Broutman, Lawrence J., Analysis and Performnace of fiber Composites, Second Edition, Wiley-Interscience Plubication, New York, pp., 125-129.

13. Dubé, M., Camoplast Composite Group, Sherbrooke, Quebec, February 2000.

14. Eckold, G., Design and manufacture of Composite Structures, McGraw-Hill Inc., New York, 1994, pp. 251-304.

15. Airtech advanced material group, Product catalogue, Huntington Beach, California.

16. Bell Helicopter, Division of Textron, Mirabel, Quebec, November 1997.

17. Beckwith, S. W., "Liquid Molding/Resin Infusion Processing Technologies", SAMPE Tutorial CFA's Composites 2000, Las Vegas, Nevada, 28 September 2000.

18. Radius Engineering inc., Composites Manufacturing Solutions, Salt Lake City, Utah, 1999.

19. Pham, X.-T., Trochu, F., Gauvin, R., "Simulation of Compression Resin Transfer Molding with Displacement Control", J. of Reinforced Plastics & Composites, 17(17): 1525-1556, 1998.

20. Trochu, F., Ferland, P., Gauvin, R., "Functional Requirements of a Simulation Software for Liquid Molding processes", Science & Engineering of Composite Materials, 6(4): 209-218, 1997.

21. Trochu, F., Hammami, A., Benoit, Y., "Prediction of Fibre Orientation and Net Shape Definition of Complex Composite Parts", composites: part a, 27(4): 319-328, 1996.

22. Terland, P., Guittard, D., Trochu, F., "Concurrent Methods for Permeability Measurement in Resin Transfer Molding», Polymer Composites, 17(1): 149-158, 1996.

23. Trochu, F., Gauvin, R., Gao, D.M., "Numerical Analysis of the Resin Transfer Molding Process by the Finite Element Method», Advances in Polymer Technology, 12(4): 329-342, 1993.

24. Columbus, High Performance Tube and Forks, Milan, Italy

25. Kestrel USA, Watsonville, California.

26. Kinesis USA, Portland, Oregon.

27. Profile Design, Carson, California.

28. Reynolds Composites, Vista, California.

29. Wound Up Composite Cycles, Salt Lake City, Utah.

30. Turner, T. J., "A Preliminary Investigation Into the Response of a Carbon Fiber Epoxy Composite Bicycle Fork to Static and Fatigue Loading", Honours Thesis, Dept. of Mechanical Engineering, McGill University, Montreal, 1997.

31. Bouraad, J., "Joining of Laminated Composite Materials with Titanium", Master's Thesis, Dept. of Mechanical Engineering, McGill University, January 1997.

32. Adams, R.D., Harris, J.A., "Bonding of Composites to Metals", Adhesion, Vol. 12, 1988.

33. Tucker, W. C., "Composite Materials Technology", American Society of Mechanical Engineers, Vol. 32, 1990, pp. 95-99.

34. Tucker, W. C., Brown. R. and Russell, L., "Corrosion Between a Graphite/Polymer Composite and Metals", Journal of Composite Materials, Vol. 24, 1990, pp. 92-102.

35. Leong, B. A., "A Testing Device for Bicycle Components", Design Project, Dept. of Mechanical Engineering, McGill University, Montreal, November 2000.

36. Dupas, C. and Senechal, J.-B., "A Testing Method for Bicycle Forks", Design Project, Dept. of Mechanical Engineering, McGill University, Montreal, June 1997.

37. Toye, Danny, et al. "Fatigue Testing Device for Bicycle Forks", Design Project, Dept. of Mechanical Engineering, McGill University, Montreal, April 2000.

38. The Advanced Composites Group, Technical manual, Tulsa, Oklahoma, 1999

39. Caniglia, R., "Applied Classical Laminate and Thin Walled Beam Theory-An Introduction to MLAM", Master's Thesis, Dept. of Mechanical Engineering, McGill University, 1992.

40. SDRC I-DEAS Master's Series V2.0, Integrated Design Engineering Software, user manual, Structural Dynamics Research Corporation, Milford, Ohio, 1994.

41. A&P Technology, The Braid Calculator, Covington, Kentucky, 1999

42. A&P Technology, Unimax™ Product Data Sheet, Covington, Kentucky, July 1998

43. A&P Technology, Gammasox™ Product Data Sheet, Covington, Kentucky, July 1998

44. Performance Polymers, Resinfusion™ Epoxies for Vacuum-Assisted Resin Transfer Molding, Ciba Specialty Chemicals, Lansing, Michigan.

45. Dow Plastics, D.E.R. 383 Product Information Form No. 296-01458-1200 WC+M, Dow Chemical Company, Midland, Michigan, December 2000.

46. Dow Plastics, D.E.H. 24 Product Information Form No. 296-01496-1200 WC+M, Dow Chemical Company, Midland, Michigan, December 2000.

47. Epoxy Products & Intermediates, Epoxy Resins Selection Guide Form No. 296-01344-498 WC+M, Dow Chemical Company, Midland, Michigan, 2000.

48. Dow Plastics, Dow Liquid Epoxy Resins Form No. 296-00224-0199 WC+M, Dow Chemical Company, Midland, Michigan, January 1999.

49. Dow Plastics, Dow Epoxy Resins Product Stewardship Manual Form No. 296-00312-898 WC+M, Dow Chemical Company, Midland, Michigan, August 1998.

50. Dow Plastics, Dow Epoxy Curing Agents Product Stewardship Manual Form No. 296-01331-292X-P&M, Dow Chemical Company, Midland, Michigan, August 1998.

51. Resolution Performance Products, EPON™ Resin 862/EPI-CURE™ Curing Agent W System Product Bulletin SC:1183-01, Houston, Texas, 2001.

52. Resolution Performance Products, Physical Properties Guide for Epoxy Resins and Related Products Product Bulletin SC:21-01, Houston, Texas, 2001.

53. Resolution Performance Products, Shell Resin Systems for Composites Applications Product Bulletin SC:2326-99, Houston, Texas, 2001.

54. MF Composites, Freeman Sheet Wax Data Sheet, St-Laurent, Quebec.

55. Ciba Speciality Chemicals, Pur-Fect Tool Data Sheet, East Lansing, Michigan.

56. Zeller International Speciality Chemical Division, Cleartex™ data sheet, Downsville, New York.

57. Rhône-Poulenc Silicones, Rhodorsil RTV-1556 product data sheet, Troy, New York.

58. Chevalier, E., Mattechk Industrie, Ste-Hippolyte, Quebec.

59. General Composites Inc., Clifton Park, New York

60. Rezba, B., Telephone Interview, General Plastics Manufacturing Company, Tacoma, Washington, July 1999.

61. Dexter Corporation Polymer Systems, Freekote®770-NC Data Sheet, Seabrook, New Hampshire.

APPENDIX A
Carbon Fibre Description

A P Technology

UNIMAX™
12K Carbon

PRODUCT CODE	AXIAL ENDS	DIAMETER		YIELD		FABRIC	WEIGHT	THICKNESS at 50% FV	
		in	mm	ft/lb	m/kg	oz/yd2	g/m2	in	mm
UNIC7519									
Best Suited for Diameter	48	0.75	19.05	39.06	26	18.8	636	0.028	0.71
Relaxed Diameter		0.38	9.65	39.06	26	37.5	1273	0.056	1.42
Maximum Diameter		1.50	38.10	39.06	26	9.4	318	0.014	0.35
UNIC15016									
Best Suited for Diameter	80	1.50	38.10	23.44	16	15.6	531	0.023	0.58
Relaxed Diameter		0.75	19.05	23.44	16	31.3	1060	0.047	1.19
Maximum Diameter		3.00	76.20	23.44	16	7.8	265	0.011	0.27
UNIC2517									
Best Suited for Diameter	144	2.50	63.50	13.02	9	16.9	573	0.025	0.63
Relaxed Diameter		1.25	31.75	13.02	9	33.8	1146	0.050	1.27
Maximum Diameter		5.00	127.00	13.02	9	8.4	287	0.012	0.30
UNIC37516									
Best Suited for Diameter	208	3.75	92.25	9.01	6	16.3	552	0.024	0.60
Relaxed Diameter		1.88	47.75	9.01	6	32.5	1103	0.049	1.24
Maximum Diameter		7.50	190.50	9.01	6	8.1	276	0.012	0.30
UNIC47517									
Best Suited for Diameter	272	4.75	120.65	6.89	5	16.8	570	0.025	0.63
Relaxed Diameter		2.38	60.45	6.89	5	33.6	1139	0.050	1.27
Maximum Diameter		9.50	241.30	6.89	5	8.4	285	0.012	0.30
Sleevings braided with 32 msi Modulus, 560 ksi tensile strength carbon axials with elastic.									

Table A.1: A&P Technology unidirectional carbon data sheet [42].

A P Technology

GAMMASOX™ Carbon Fiber Braids

PRODUCT CODE	DIAMETER		ANGLE	YIELD		FABRIC	WEIGHT	THICKNESS at 50% FV	
	in	mm	+/-	ft/lb	m/kg	oz/yd²	g/m²	in	mm
LIGHT FABRICS									
E58L25X	0.25	6.4	45	265.2	178	8.3	281	0.013	0.33
J58L50X	0.50	12.7	45	132.6	89	8.3	281	0.013	0.33
P58L75X	0.75	19.1	45	82.9	56	8.9	302	0.013	0.33
S58L100X	1.00	25.4	45	66.3	45	8.3	281	0.013	0.33
T58L125X	1.25	31.8	45	55.2	37	8.0	271	0.012	0.30
U58L150X	1.50	38.1	45	44.2	30	8.3	281	0.013	0.33
V58L200X	2.00	50.8	45	36.8	25	7.5	254	0.011	0.28
MEDIUM FABRICS									
H57L50X	0.50	12.7	45	82.9	56	13.3	451	0.020	0.51
L57L75X	0.75	19.1	45	55.2	37	13.3	451	0.020	0.51
P57L100X	1.00	25.4	45	41.4	28	13.3	451	0.020	0.51
S57L125X	1.25	31.8	45	33.1	22	13.3	451	0.020	0.51
T57L150X	1.50	38.1	45	27.6	19	13.3	451	0.020	0.51
U57L200X	2.00	50.8	45	22.1	15	12.4	420	0.018	0.46
V57L250X	2.50	63.5	45	18.4	12	11.9	403	0.018	0.46
HEAVY FABRICS									
I56L75X	0.75	19.1	45	36.8	25	19.9	675	0.030	0.76
L56L100X	1.00	25.4	45	27.6	19	19.9	675	0.030	0.76
P56L125X	1.25	31.8	45	20.7	14	21.2	719	0.032	0.81
Q56L150X	1.50	38.1	45	18.4	12	19.9	675	0.030	0.76
T56L200X	2.00	50.8	45	13.8	9	19.9	675	0.030	0.76
U56L250X	2.50	63.5	45	11.0	7	19.9	675	0.030	0.76
V56L300X	3.00	76.2	45	9.2	6	19.9	675	0.030	0.76
Sleevings braided with 32 msi modulus, 560 ksi tensile modulus carbon.									

Table A.2: A&P Technology carbon braid data sheet [43].